Neural Network Potentials to explore the Crystal Structure Landscape

Stefano de Gironcoli
Scuola Internazionale Superiore di Studi Avanzati
Trieste-Italy

Credits:

Emine Kucukbenli, Boston U (MA, USA)

Ruggero Lot, SISSA Trieste (I)

Franco Pellegrini, SISSA Trieste (I)

Yusuf Shaidu, Berkeley (CA, USA)

PANNA

Properties from Artificial Neural Network Architectures

https://gitlab.com/pannadevs/panna

CSP is a formidable task

- CSP problem: Name a chemical or stoichiometric formula; find the (local) minima of the free energy landscape under given thermodynamic conditions (often at certain T,P)
- “What is the most stable structure of glycine at ambient conditions?” “What is the carbon structure that is stable at very high pressures”
- Challenges:
  - A very vast space of possibilities.
  - Free energy landscape is very expensive to obtain accurately

ζ-Glycine: Insight into the mechanism of a polymorphic phase transition

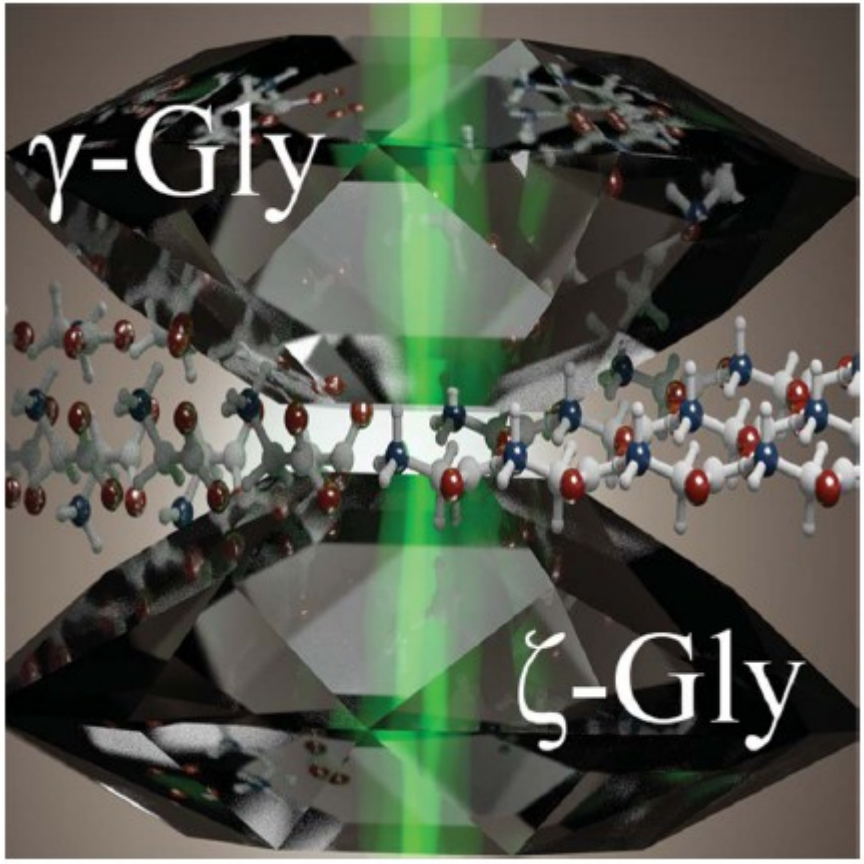

Glycine

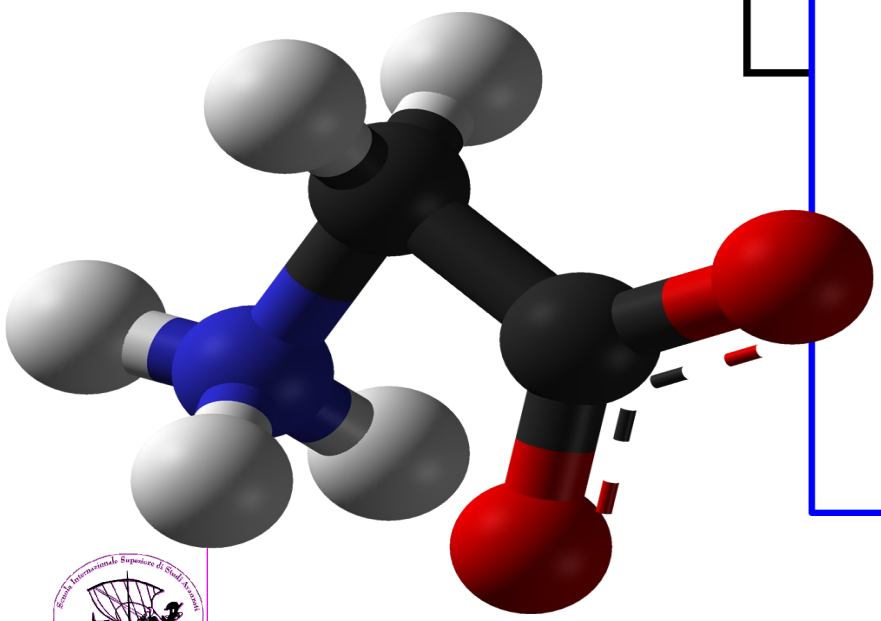

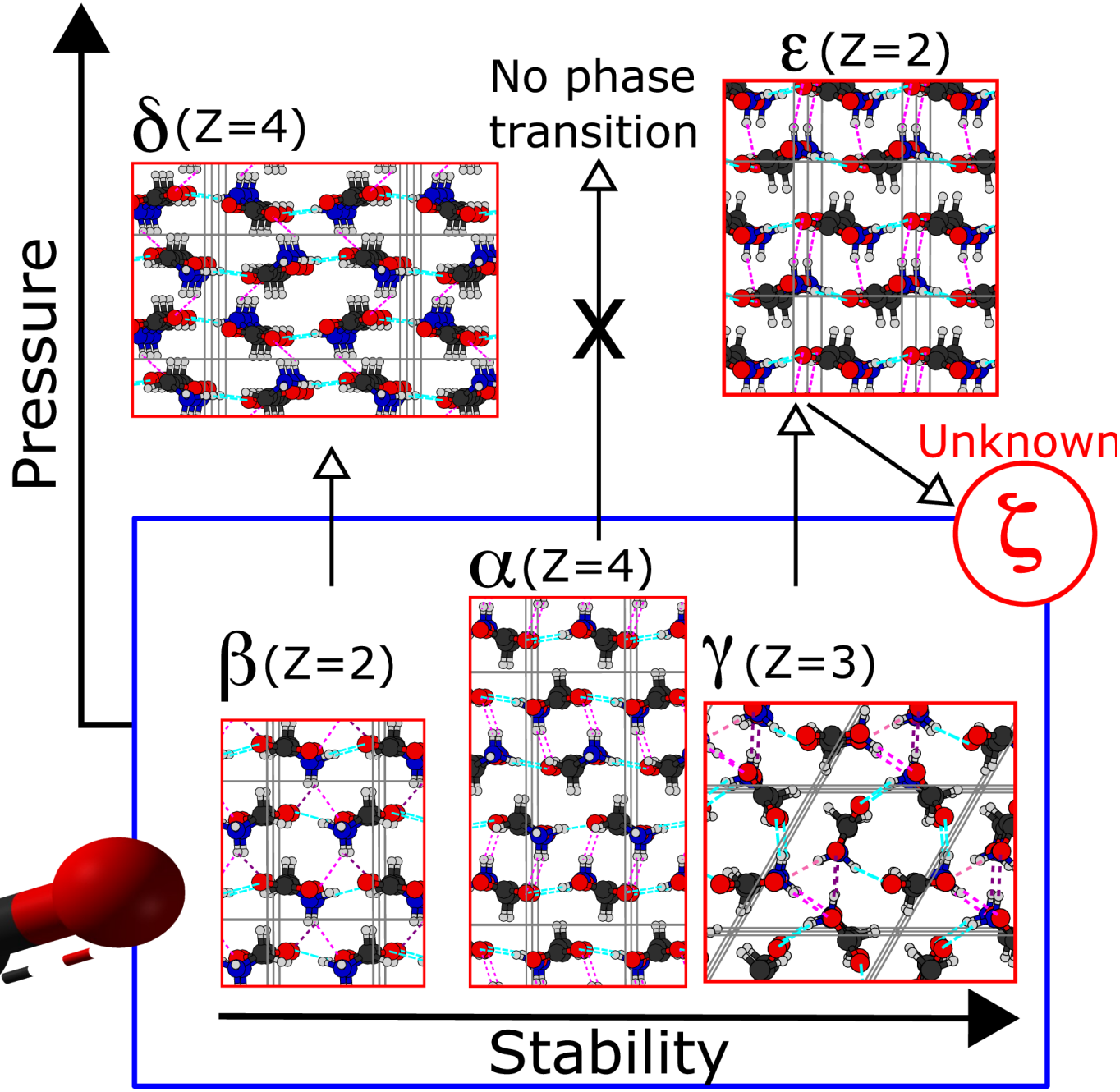
Pressure
δ(Z=4)
No phase transition
ε(Z=2)
Unknown
ζ
α(Z=4)
β(Z=2)
γ(Z=3)
Stability

How to tackle CSP?

Explore: Use smart algorithms to explore as much of the landscape as possible

Molecular dynamics / Monte Carlo walkers

- Simulated annealing
- Metadynamics
- Basin hopping
- Minima hopping
- Genetic algorithm

Genetic algorithm

(a) heredity

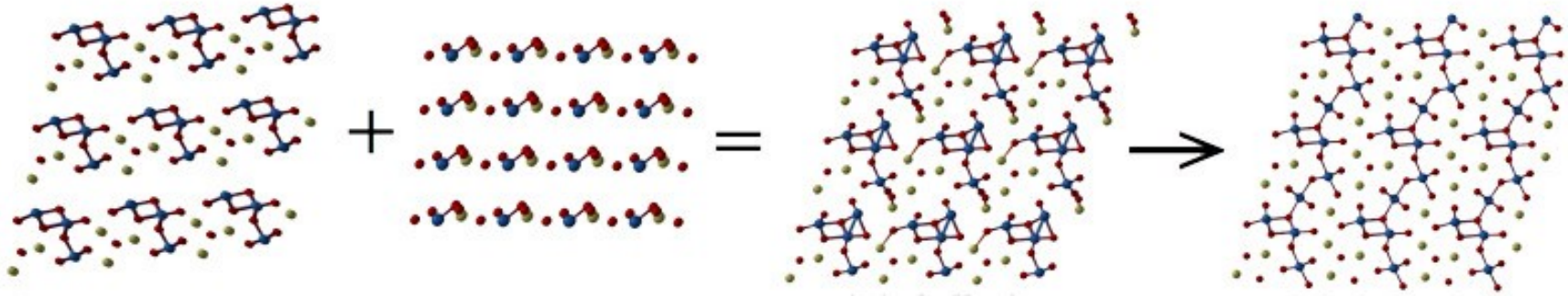

slice from parent #1 slice from parent #2 non-optimized offspring optimized offspring

(b) lattice mutation

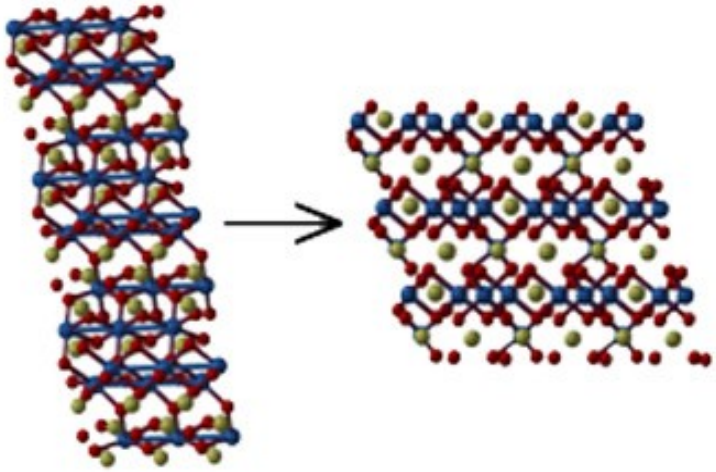

(c) softmode mutation

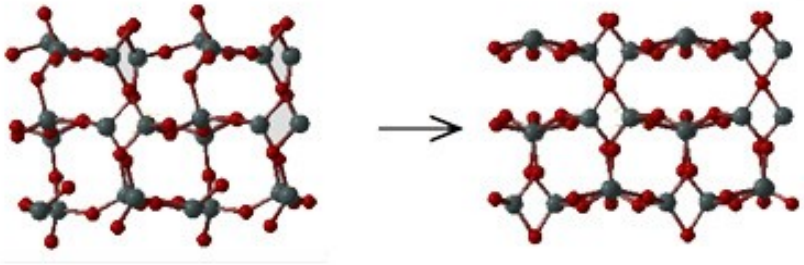

(d) permutation

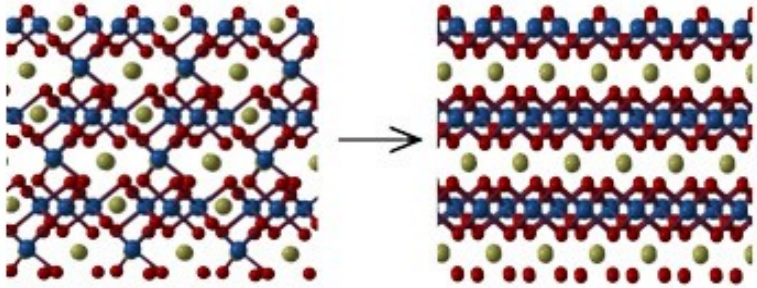

USPEX operations

USPEX + QUANTUM ESPRESSO

+ vdWDF + clustering

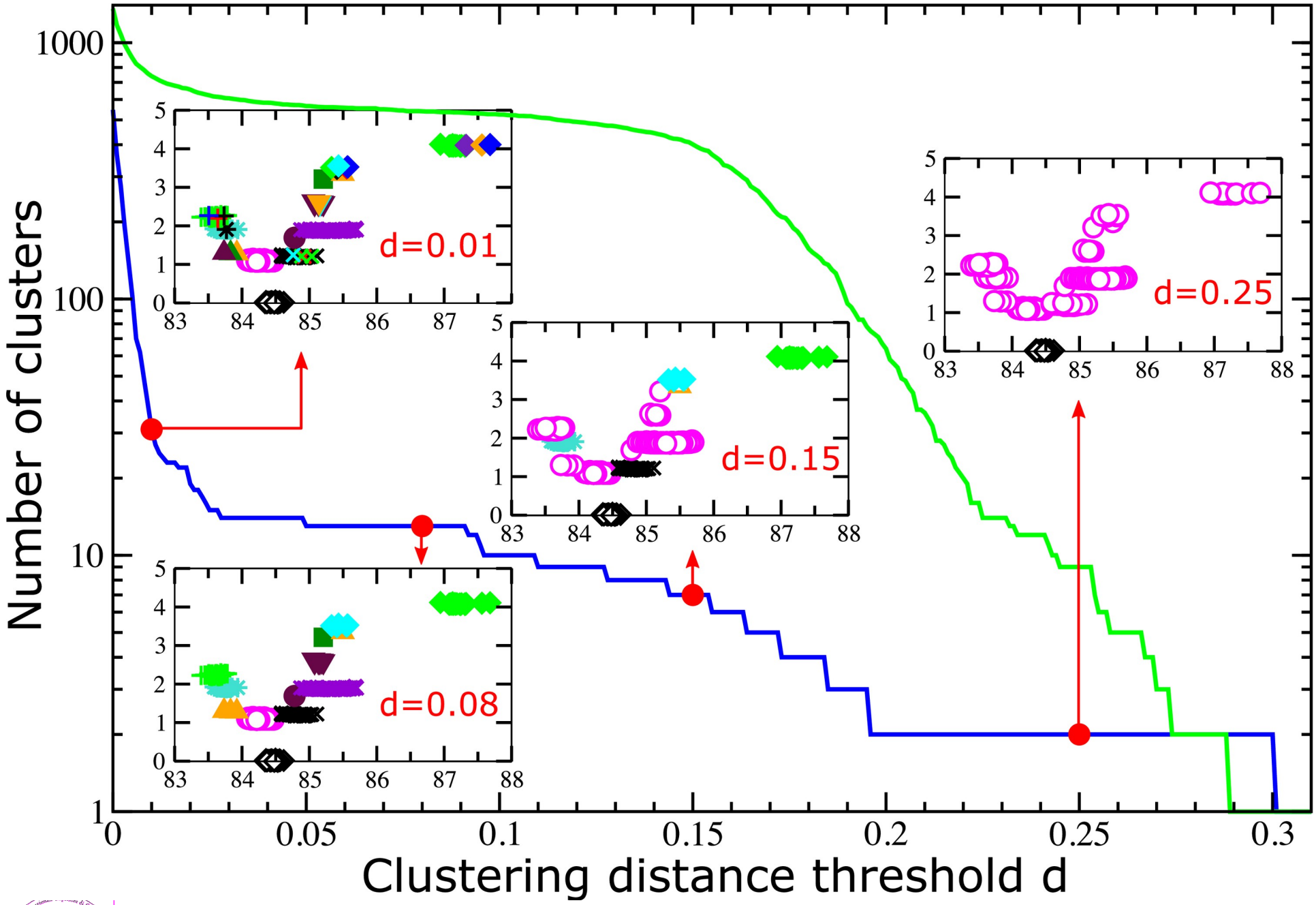
Number of clusters
Clustering distance threshold d
1000
100
10
1
0
0.05
0.1
0.15
0.2
0.25
0.3
d=0.01
d=0.08
d=0.15
d=0.25

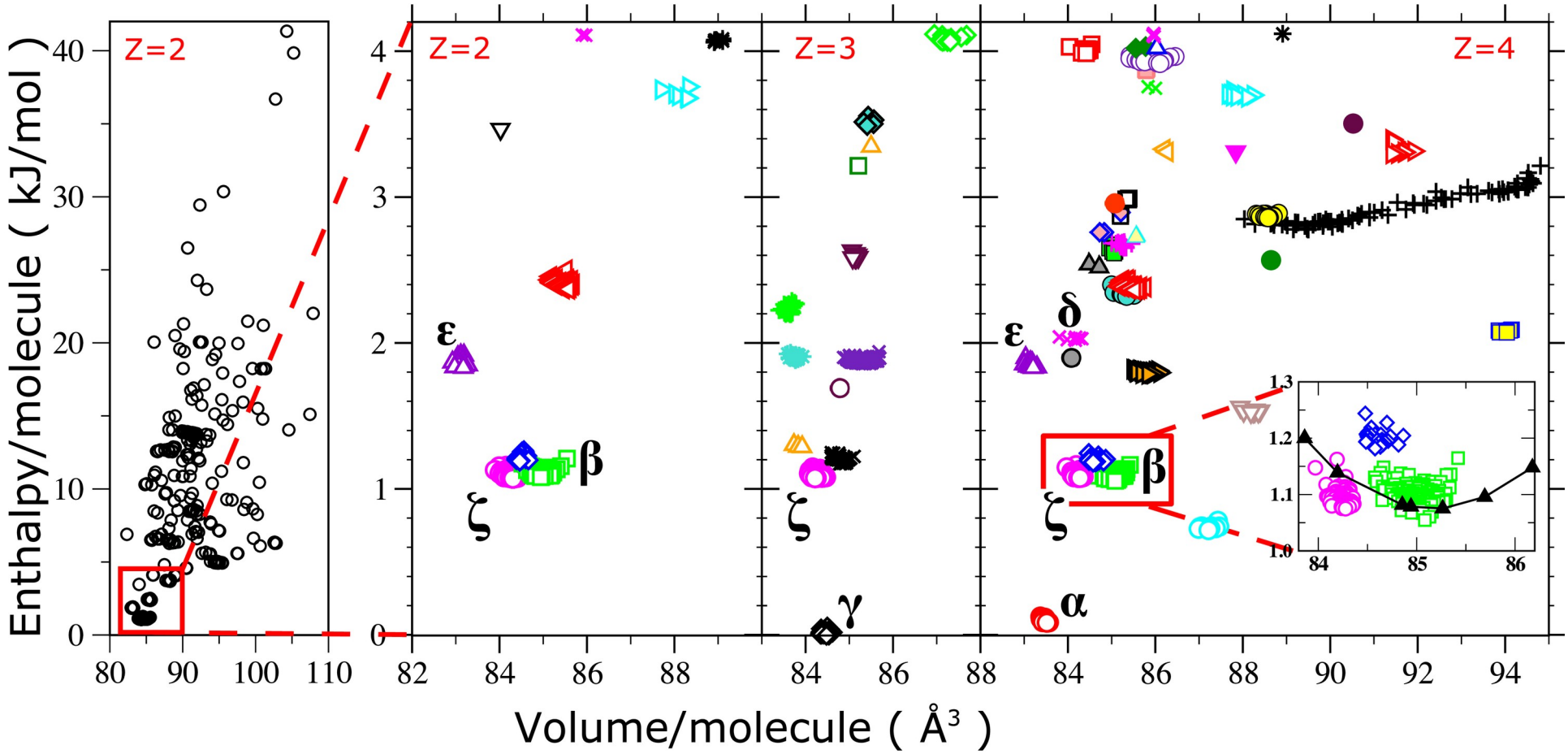
Z=2
Z=2
Z=3
Z=4
Enthalpy/molecule (kJ/mol)
Volume/molecule (Å³)
ε
β
ζ
γ
δ
α

ζ-phase

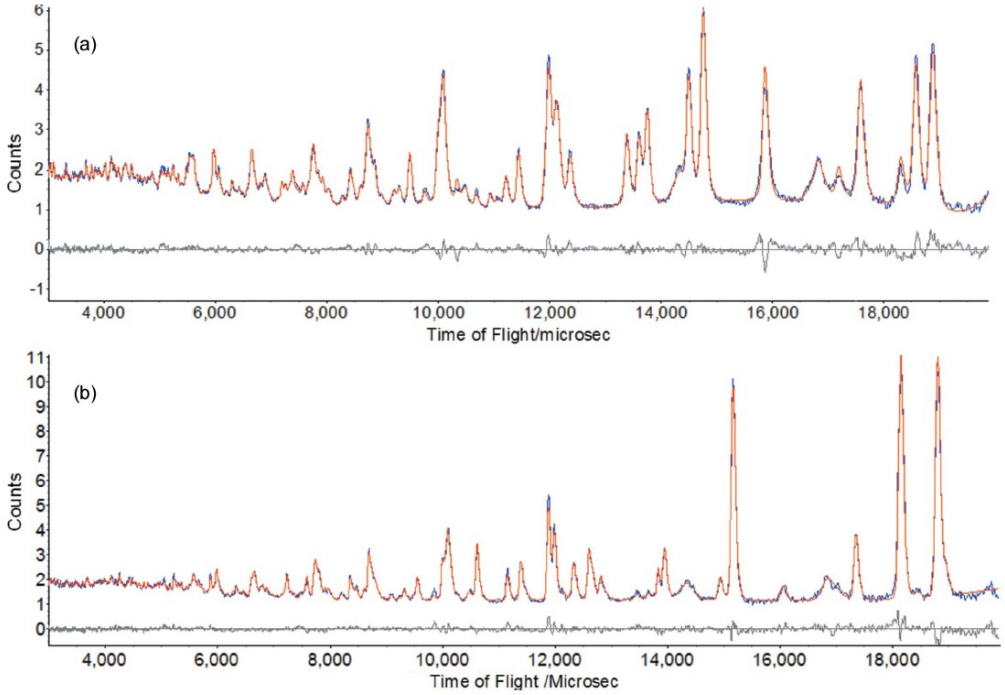

Figure 2
(*a*) Rietveld fit of the neutron powder diffraction pattern of ζ-glycine at 100 K (blue = observed, red = calculated). In addition to the peaks ζ-glycine, the pattern also shows the presence of residual ε- and a trace of γ-glycine. Other peaks arise from the sample environment, namely th pressure marker and the Al_2O_3 and ZrO_2 components of the anvils of the pressure cell. (*b*) Rietveld fit of the neutron powder diffraction patte β-glycine (contaminated with ζ- and a trace of γ-glycine) at 290 K. A 1 Å *d* spacing approximates to 4837 μs in time-of-flight.

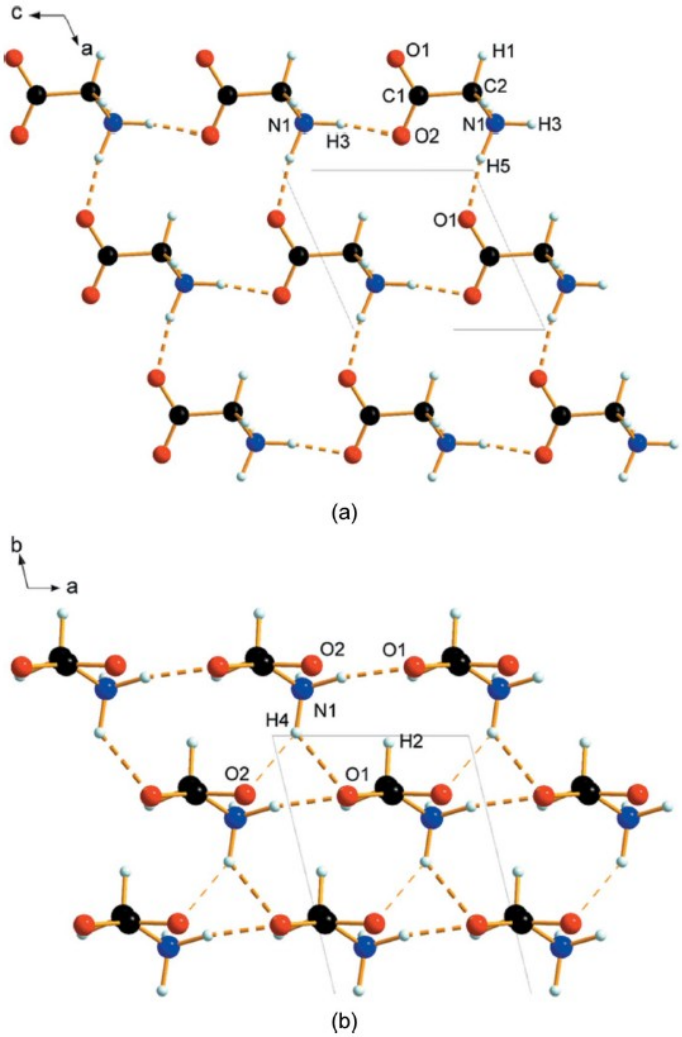

Figure 3
Intermolecular interactions in ζ-glycine. (*a*) Layers formed in the *ac* plane, viewed along **b**. (*b*) Stacking of the layers, viewed along **c**.

E Kucukbenli, CH Pham, SdG,
C Bull, G Flowitt-Hill, HY Playford, M Tucker, S Parsons
Int Union Crist J **4**, 569–574 (2017)

Exploring the phase space for larger molecules (ex. CLR) requires fast and accurate energetics

Complete ^{13}C Chemical Shift Assignment for Cholesterol Crystal

ζ-Glycine: Insight into the mechanism of a polymorphic phase transition

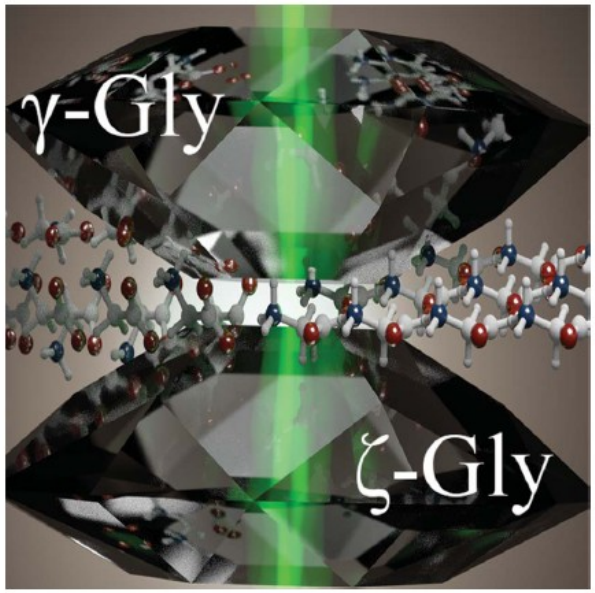

Lithium-ion Batteries

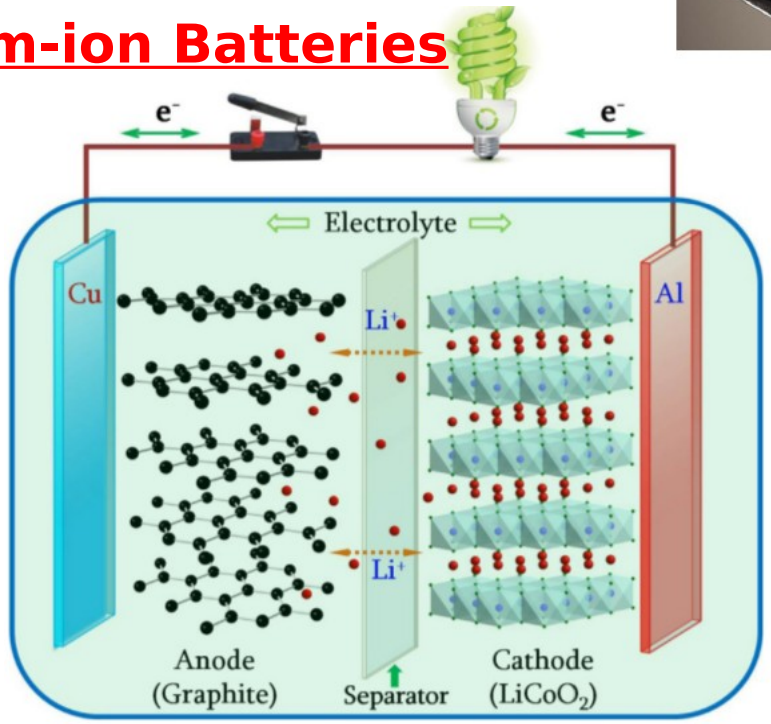

Why Cholesterol ?

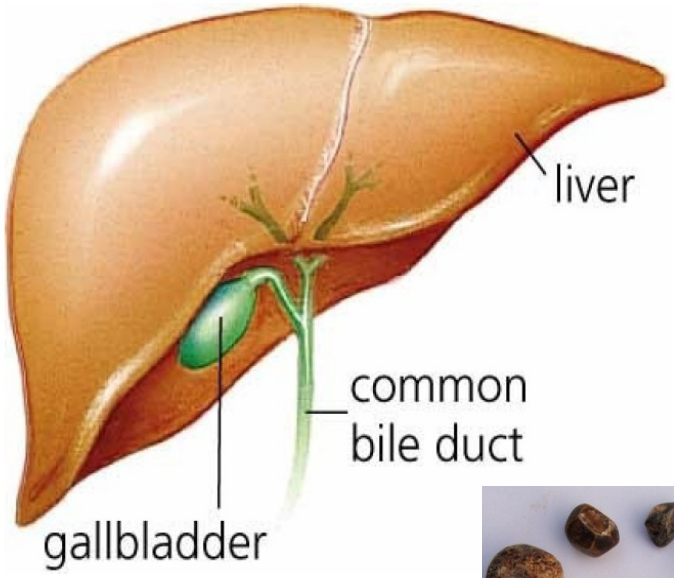

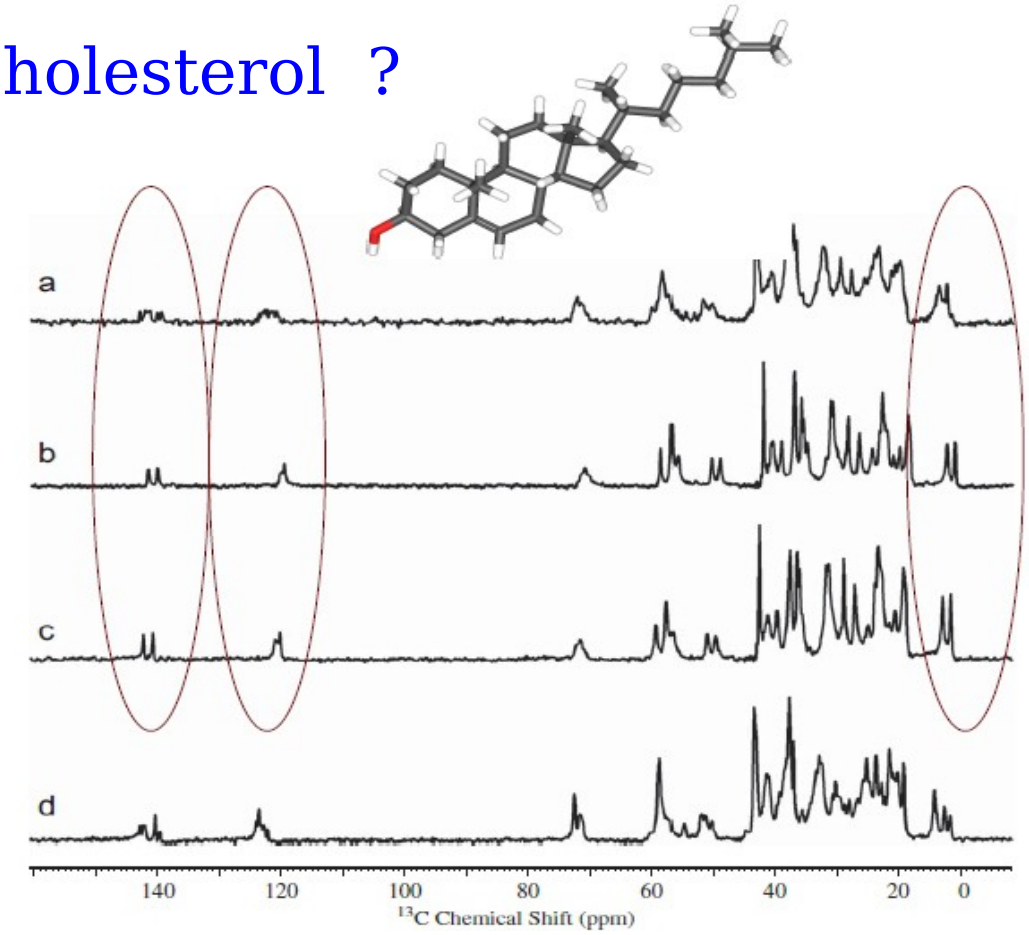

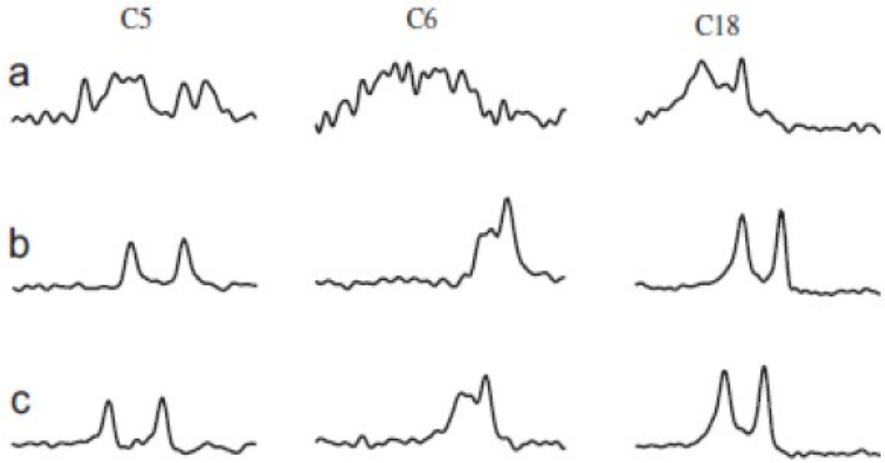

a) Gallbladder Cancer

b) Chronic Cholecystitis

c) Xantho-Granulomatous Cholecystitis

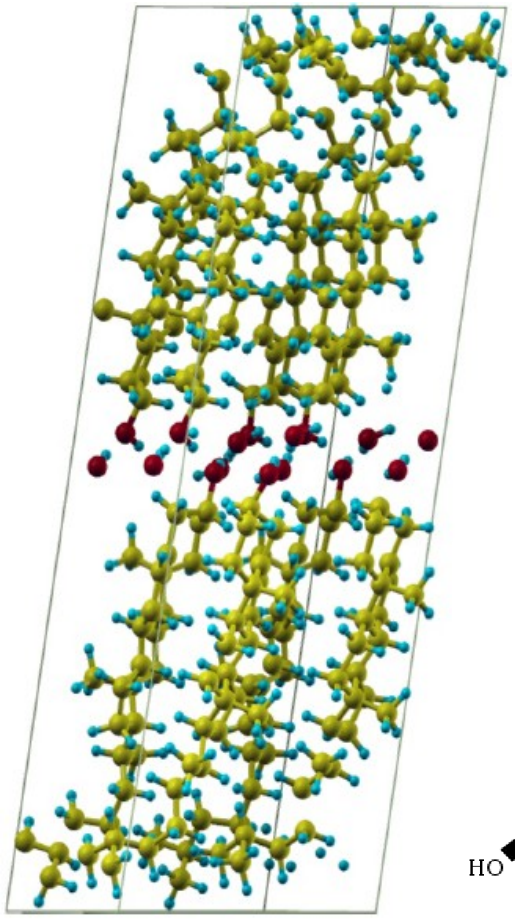

Monohydrade Cholesterol (ChM)
8 CLR +8 w molecules - 616 atoms

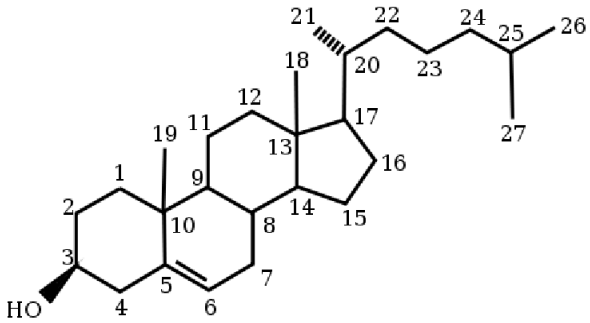

High temperature Anhydrous Cholesterol (ChAh)
16 CLR mol – 1184 atoms

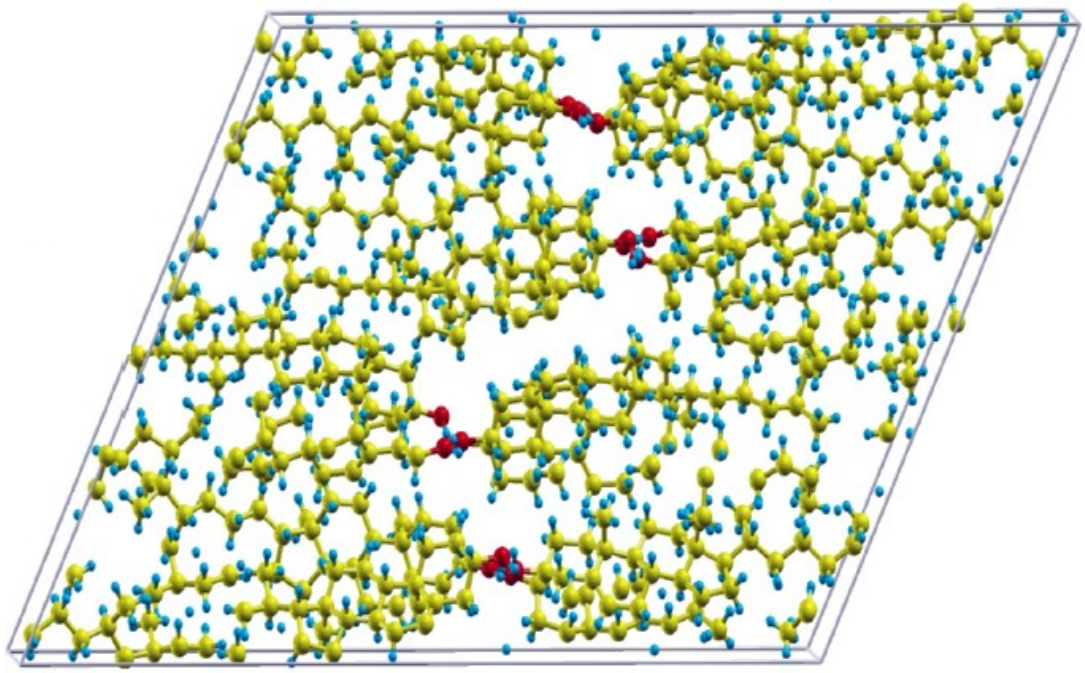

Low temperature Anhydrous Cholesterol (ChAl)
8 CLR mol – 592 atoms

(not shown)

Lithium Interaction with Graphene-like Materials

~10Wh ~100Wh ~10,000Wh

Lithium ion batteries

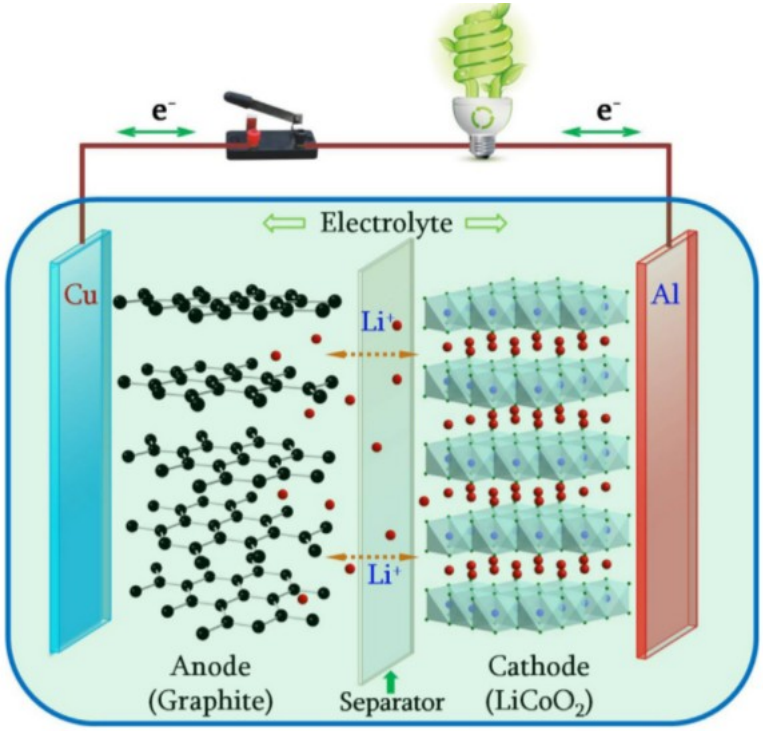

- Cathode: Source of lithium
- Electrolyte: Ionic conductivity
- Anode: Lithium holder
- Current collectors

Materials Today 19(2):109-123, 2016

Capacity: The amount of Li absorbed by anode

- Stoichiometry of Li adsorbed graphite is LiC_6

Alternative anode materials :

Graphene due to its large surface to mass ratio and good electrical conductivity.

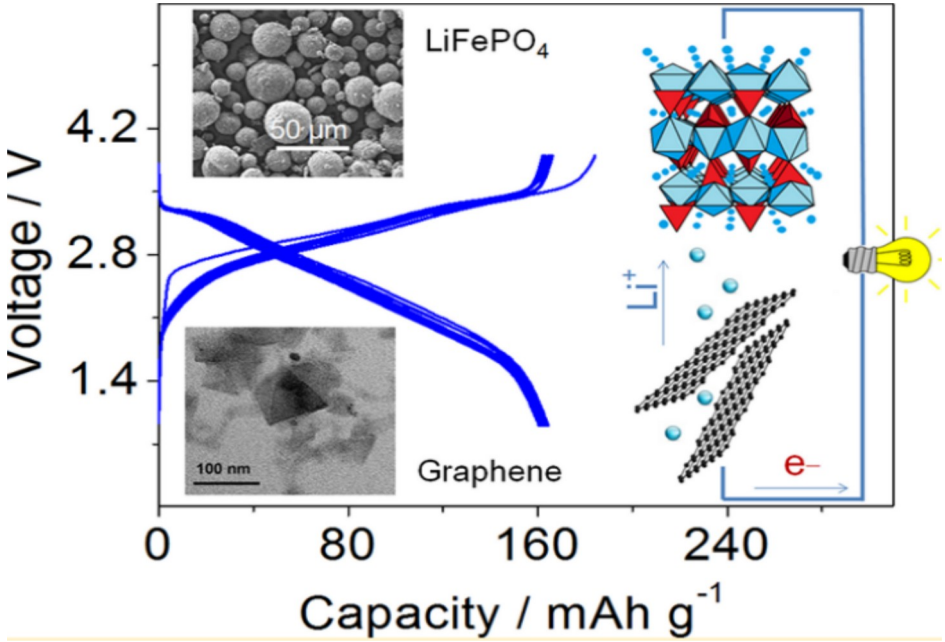

- graphene nanoflakes as alternative anode
- Flakes ~30-100 nm lateral dimension
- **Very high Li uptake: LiC_2**

Hassoun et al. Nano Lett. 2014, 14, 4901-4906

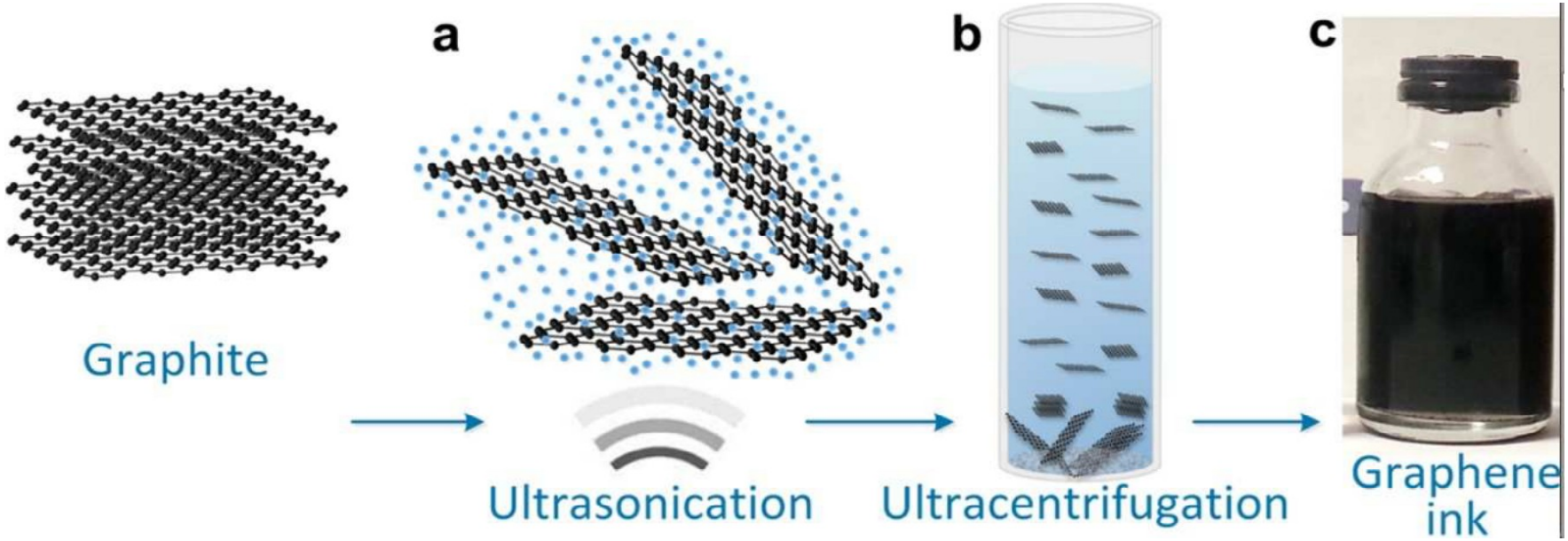
a
b
c
Graphite
Ultrasonication
Ultracentrifugation
Graphene ink

Traditionally model potentials construction requires a lot of physical intuition and are strongly dependent on the available experimental information.

Not transferable to experimentally unexplored regions.

Limited accuracy due to rigid functional form.

DFT is a viable option to gather accurate information but requires a systematic approach to build a potential that can incorporate its features.


Artificial
Intelligence
is better than non

Replace the expensive DFT total energy calculations (or other accurate methods) with an interatomic potentials built to reproduce DFT data in a variety of environments

$$E(c) = \sum_{\alpha} \sum_{i \in \alpha} \varepsilon_{\alpha}(\mathbf{d}_i) + \cancel{\text{ long range contrib}}$$

- Kernel Ridge Regression (and Gaussian Processes)

- Neural Networks

- local environment descriptors

- Modified Behler-Parrinello descriptor

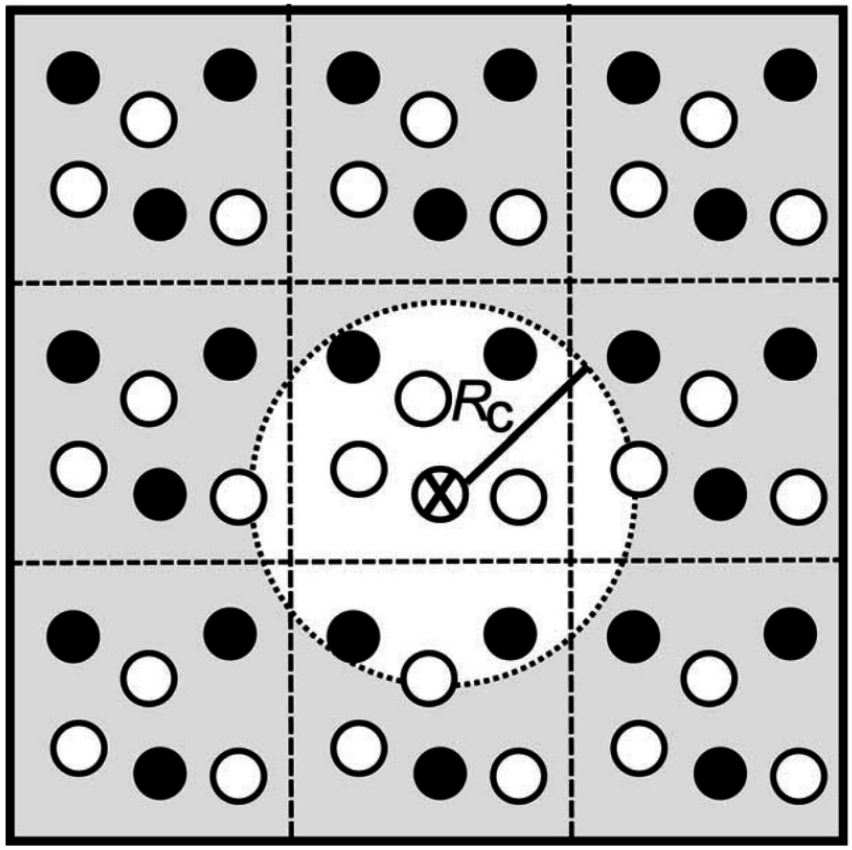

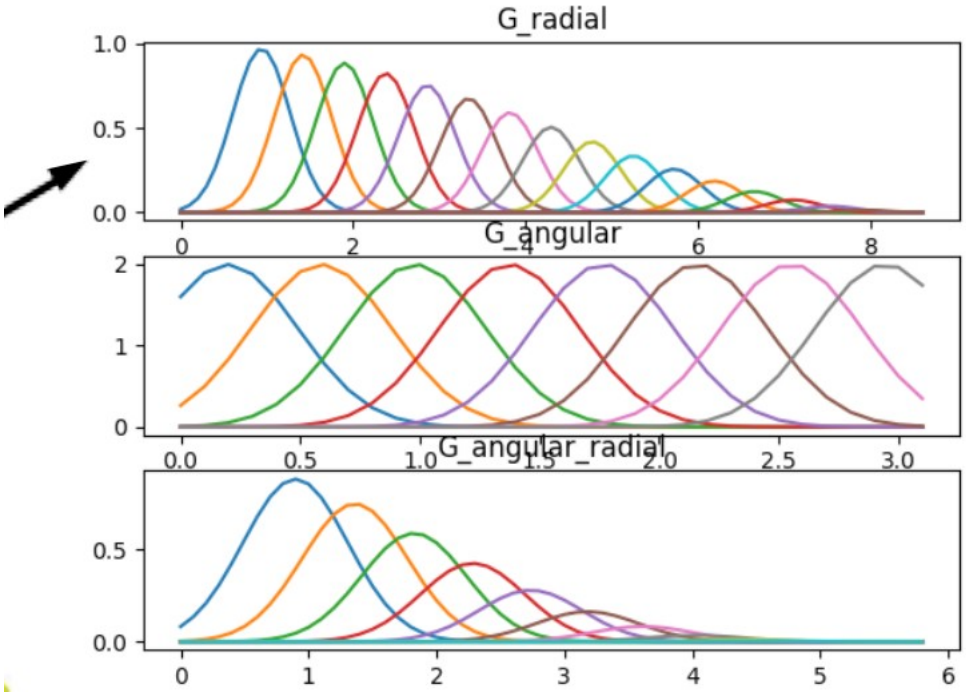

Symmetry Functions

The radial part

$$G^R = \sum_{j \neq i} e^{-\eta(R_{ij}-R_s)^2} f_c(R_{ij})$$

The angular part

$$G^A = 2^{1-\xi} \sum_{jk \neq i} (1 + cos(\theta_{ijk} - \theta_s))^{\xi} \, e^{-\eta(\frac{R_{ij}+R_{ik}}{2} - R_s)^2} f_c(R_{ij}) f_c(R_{ik})$$

$$f_c(R) = \frac{1}{2}(1 + cos(\frac{\pi R}{R_c}))$$

J. Behler and M. Parrinello, Phys. Rev. Lett. **98**, 146401 (2007)
J.S.Smith, O.Isayev and A.E.Roitberg, Chem. Sci., 2017, **8**, 3192-3203

Representation

$$G^R_{m,s;i} = \sum_{i \neq j}^{\text{All atoms kind s}} e^{-\eta(r_{ij}-R_m)^2} f_c(r_{ij})$$

$$f_c(r_{ij}) = \begin{cases} 0.5\left[\cos\left(\frac{\pi r_{ij}}{R_c}\right)+1\right] & \text{if } r_{ij} \leq R_c \\ 0 & \text{if } r_{ij} \geq R_c \end{cases}$$

R0=0.5A , Rc= 4.6A
32 bins per pair:
32x4=128 parameters

J. Behler and M. Parrinello, PRL, 98.14 (2007).

Smith et al, Chem Sci 8 3192 (2017)
DOI: 10.1039/c6sc05720a

Average G-radial for N in GLY

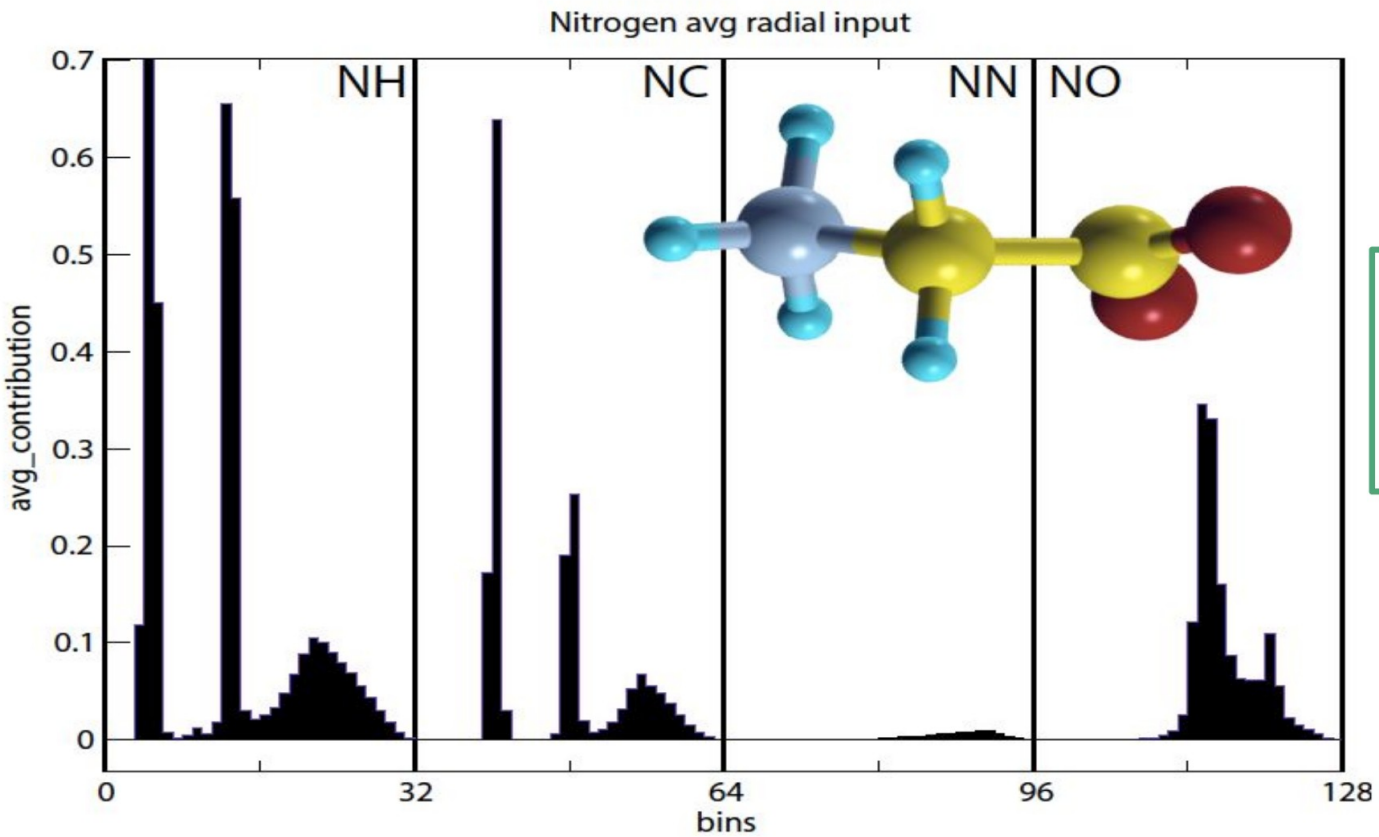

R0=0.5A , Rc= 4.6A
32 bins per pair:
32x4=128 parameters

Representation

$$G^{A}_{n,m,s;i} = 2^{1-\xi} \sum_{j,k \neq i}^{\text{All atom of kind s}} (1 + \lambda cos(\Theta_{ijk} - \Theta_n))^{\xi} e^{-\eta\left(\frac{r_{ij}+r_{ik}}{2} - R_m\right)^2} f_c(r_{ij}) f_c(r_{ik})$$

R0=0.5A , Rc= 3.1A
8 angular bin for each 8 radial bin
64 bins per trimer:
64x10=640 parameters

Smith et al, Chem Sci (2016)
DOI: 10.1039/c6sc05720a

Average G-angular in GLY

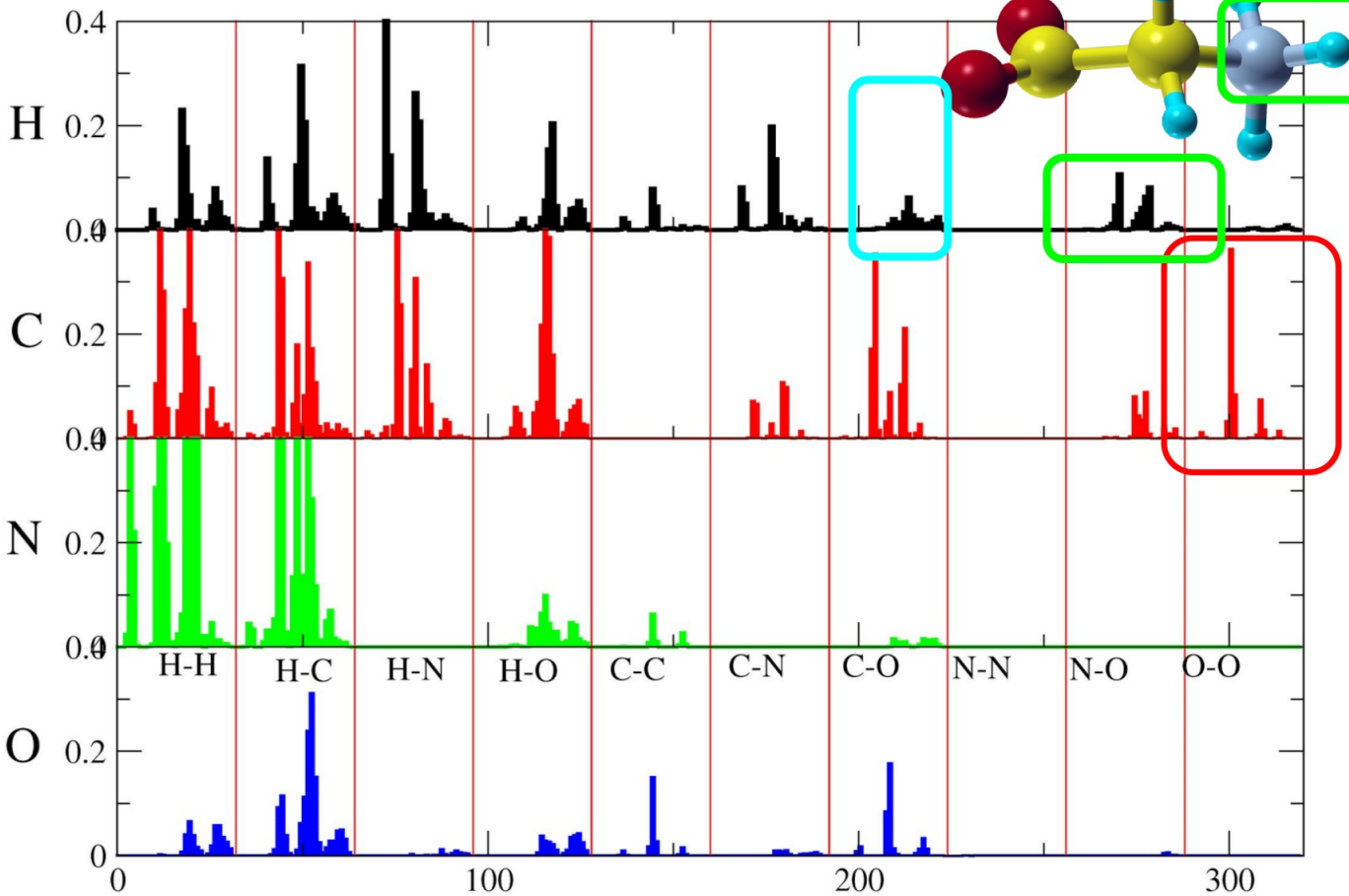

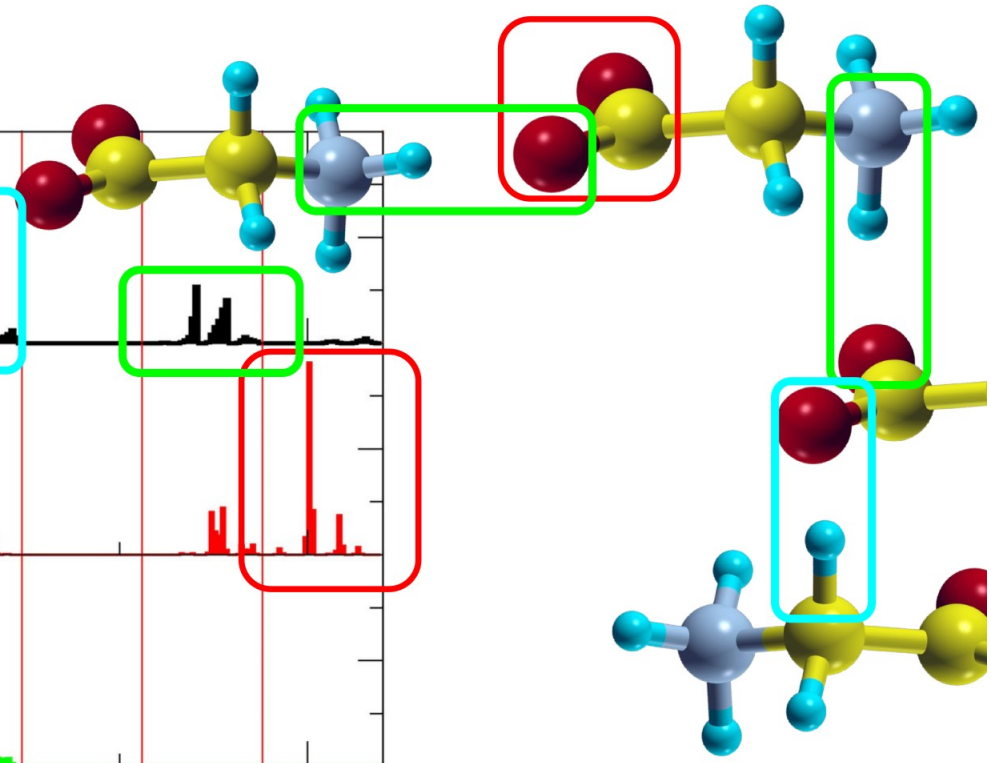

Halved version:
8 angular for 4 radial
32 per trimer
32x10=320 parameters

GLY

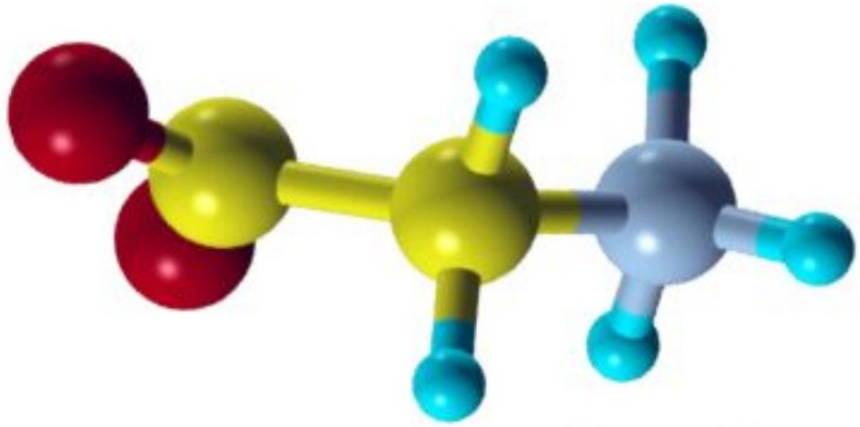

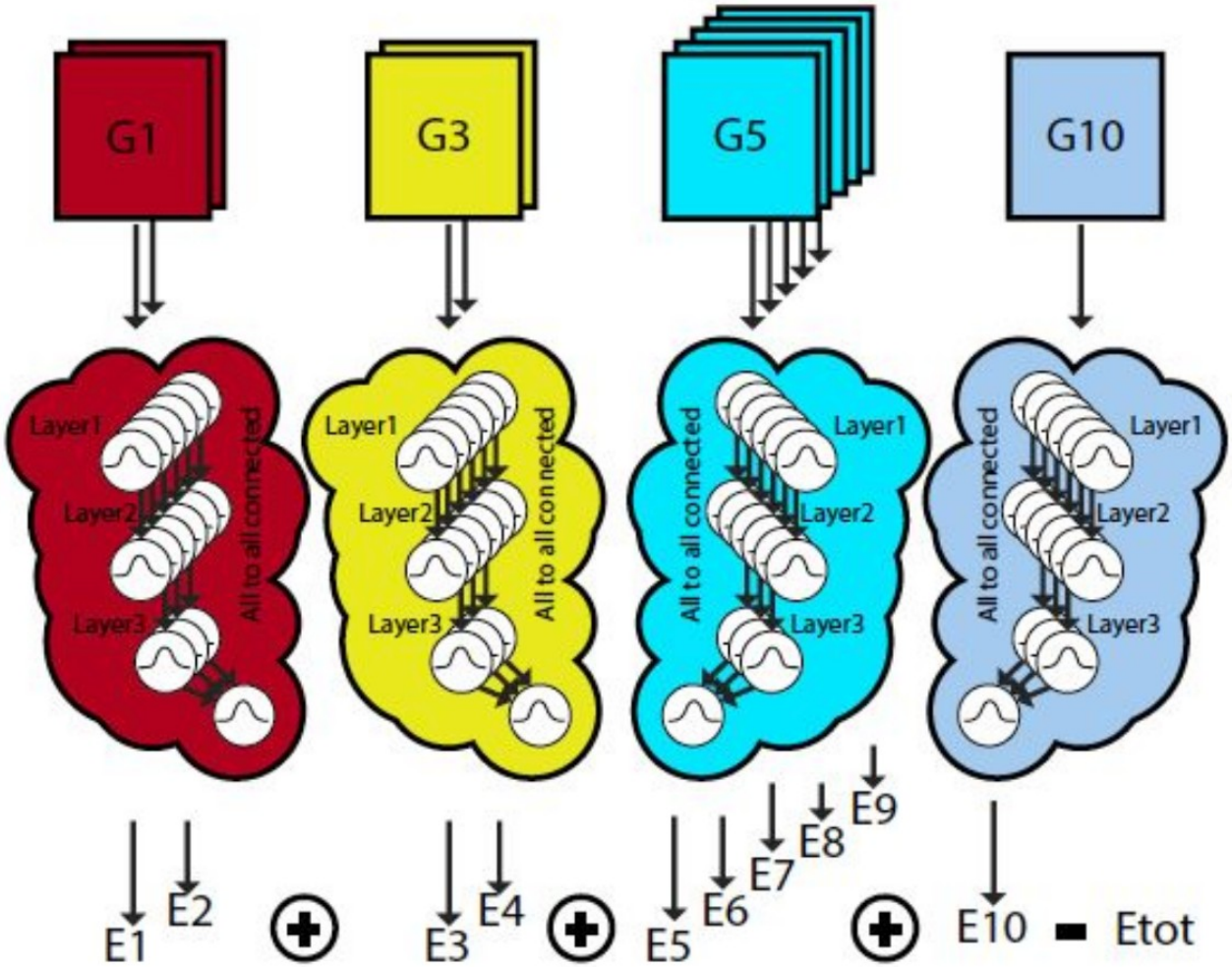
G1
G3
G5
G10
Layer1
Layer2
Layer3
All to all connected
E1
E2
E3
E4
E5
E6
E7
E8
E9
E10
Etot

PANNA workflow

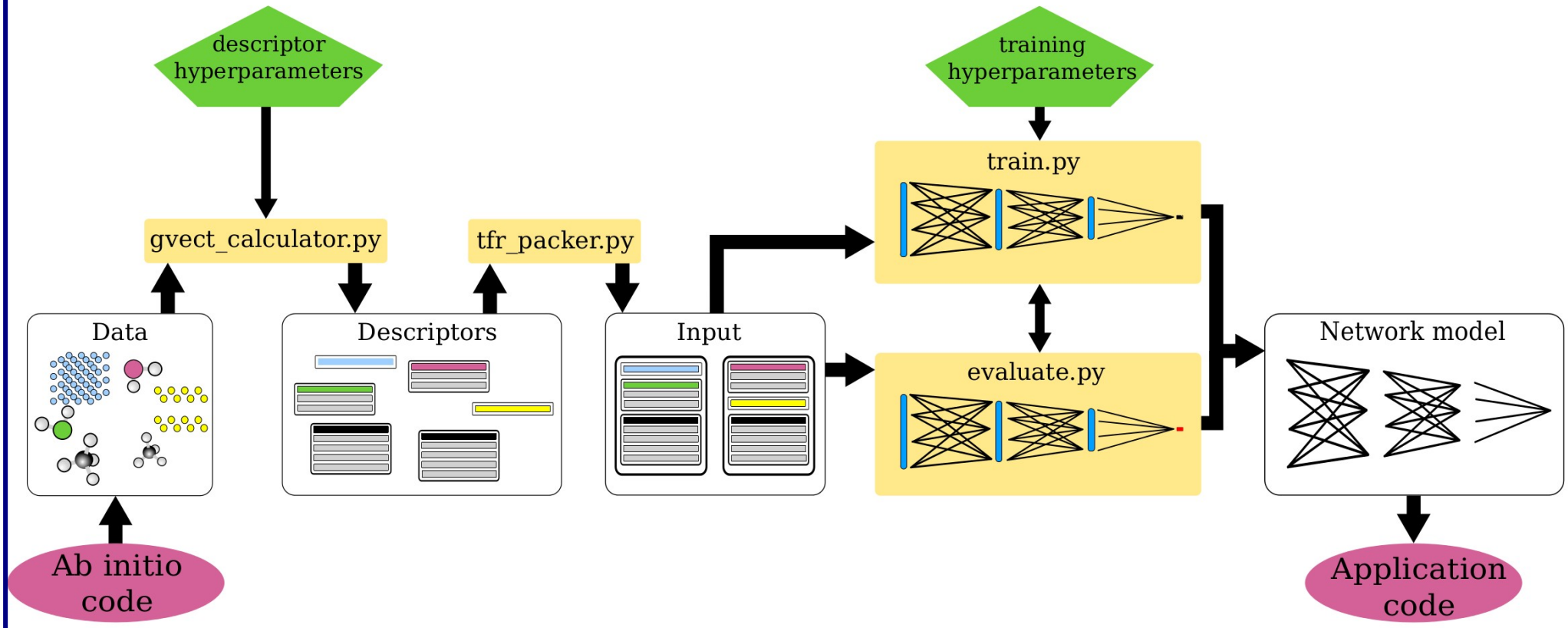

R Lot, F Pellegrini, Y Shaidu, E Kucukbenli, *arXiv:1907.03055*

https://gitlab.com/pannadevs/panna

Lithium ion batteries

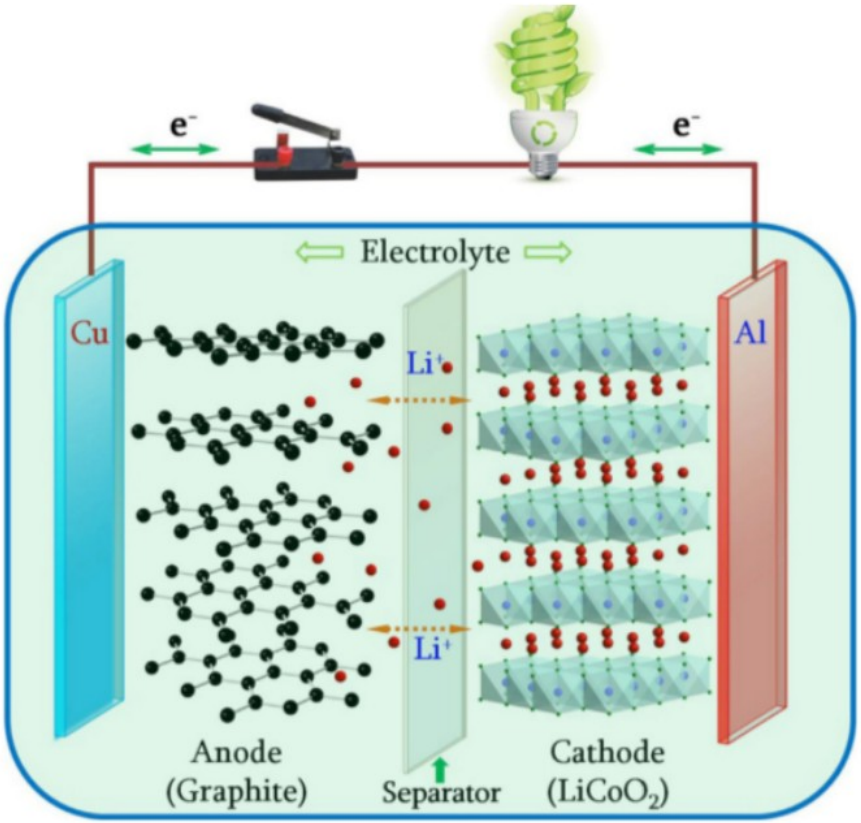

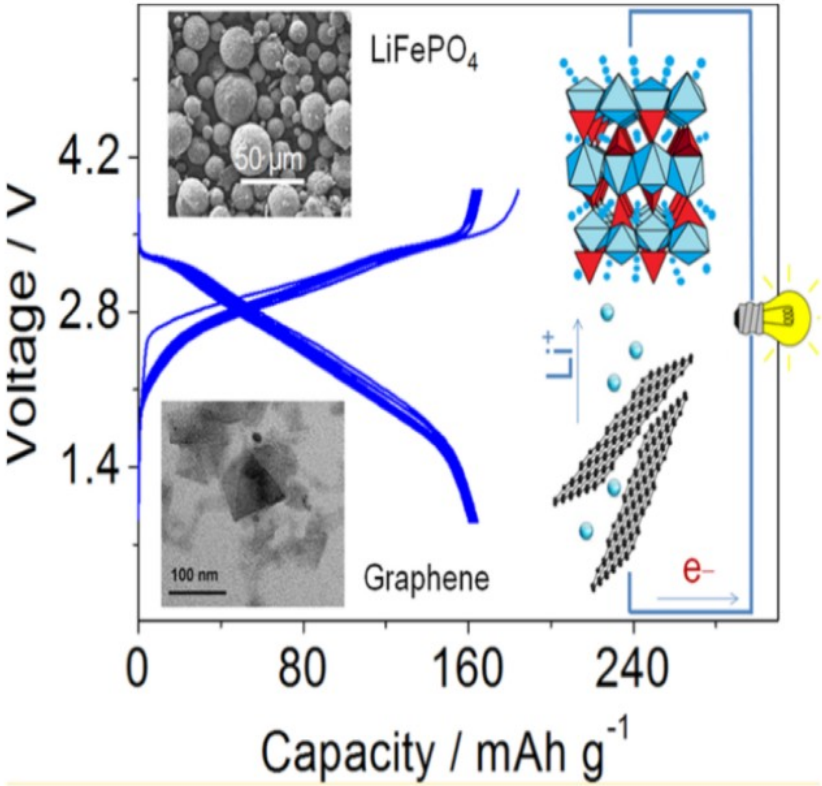

- graphite: LiC_6

Today 19(2):109-123, 2016

- graphene: LiC_2

Hassoun et al. Nano Lett. 2014, 14, 4901-4906

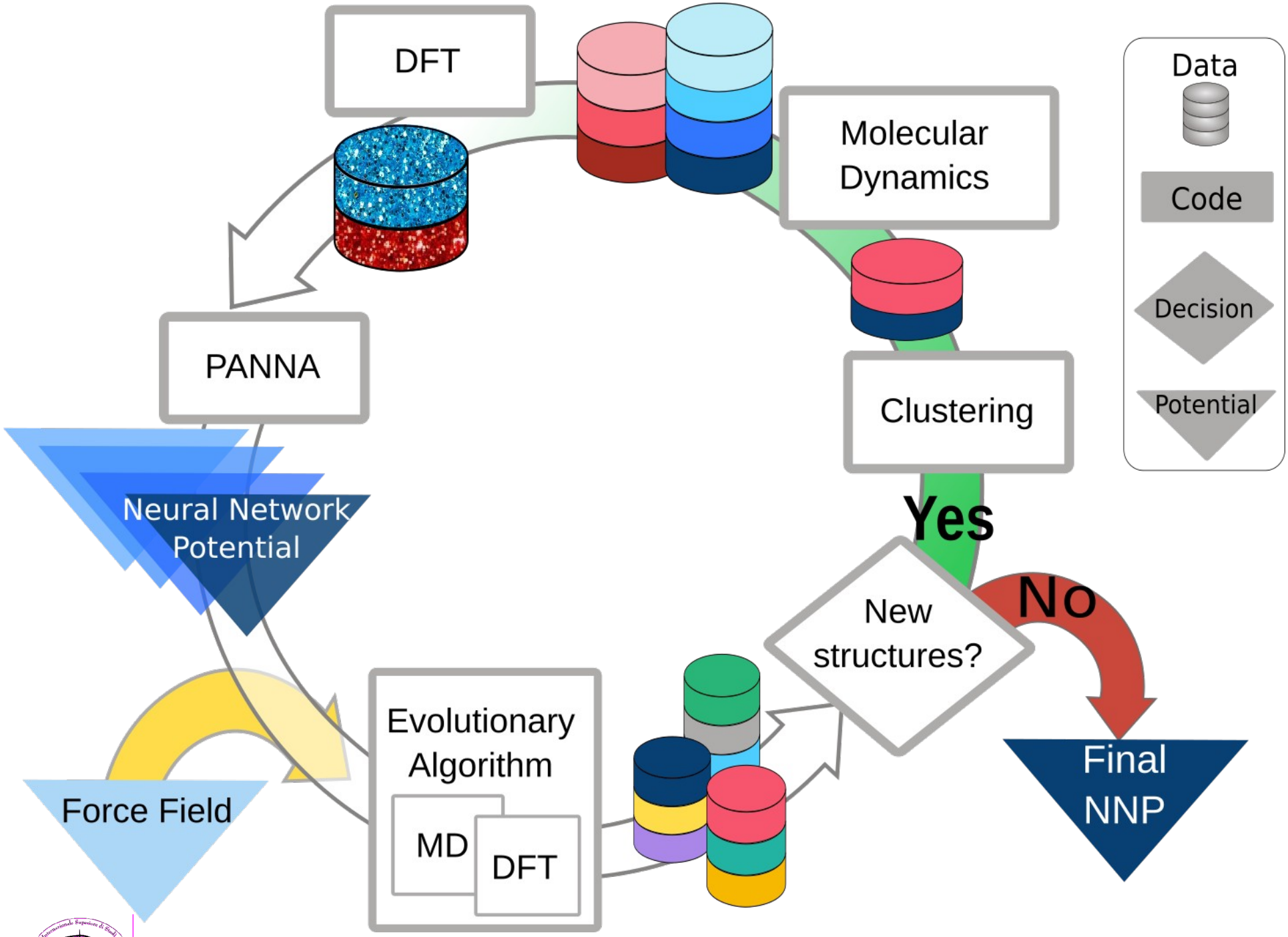
DFT
Molecular Dynamics
Data
Code
Decision
Potential
PANNA
Clustering
Neural Network Potential
Yes
No
New structures?
Evolutionary Algorithm
MD
DFT
Force Field
Final NNP

Carbon Systems

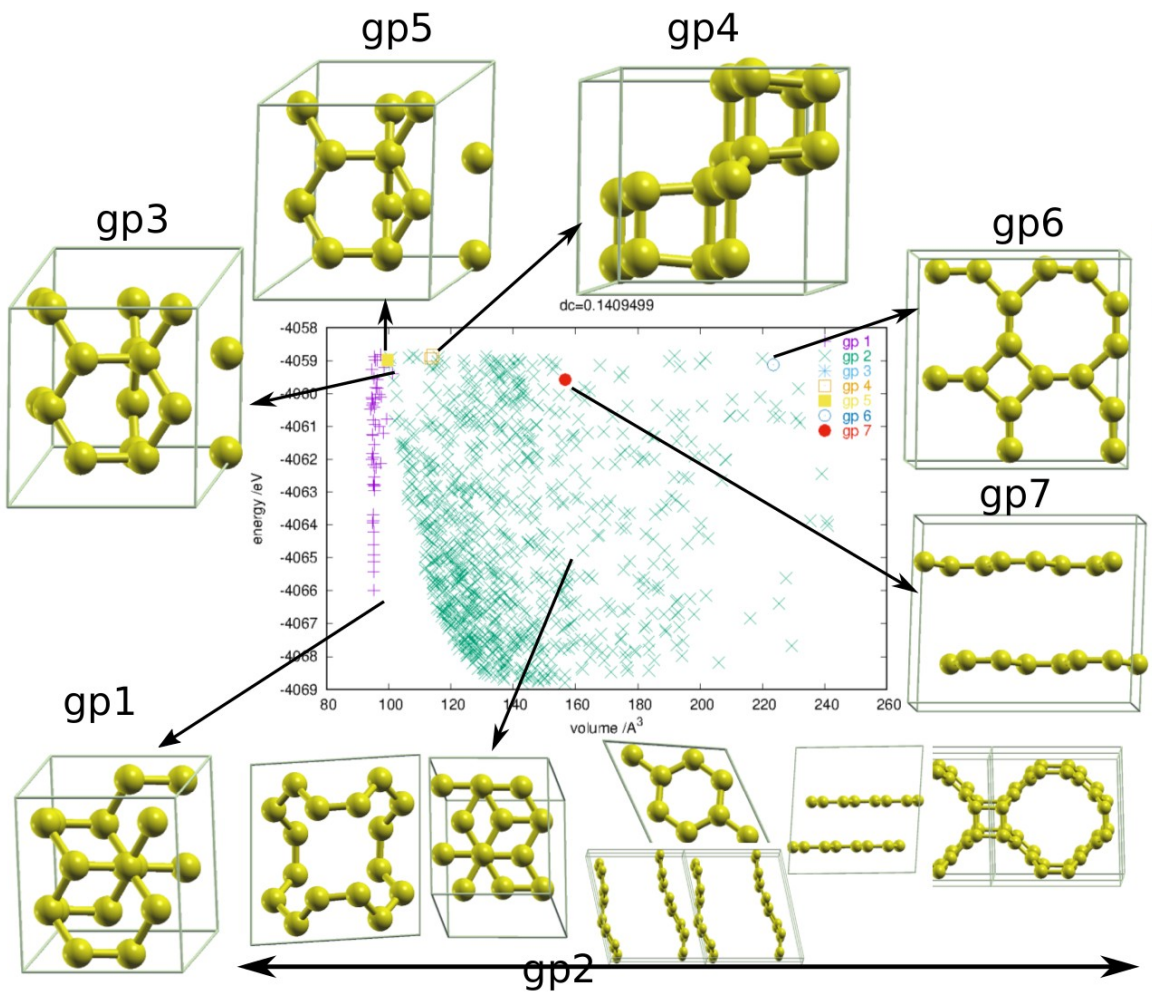

$$D = \frac{1}{2}\left(1 - \frac{\mathbf{F_1} * \mathbf{F_2}}{|\mathbf{F_1}||\mathbf{F_2}|}\right)$$

Training Parameters

- Architectures: 144:64:32:1
- Activation function: gaussian:gaussian:linear
- minimized quantity: $Loss = E_{Loss} + \beta F_{Loss}$

Carbon Systems: training and validation

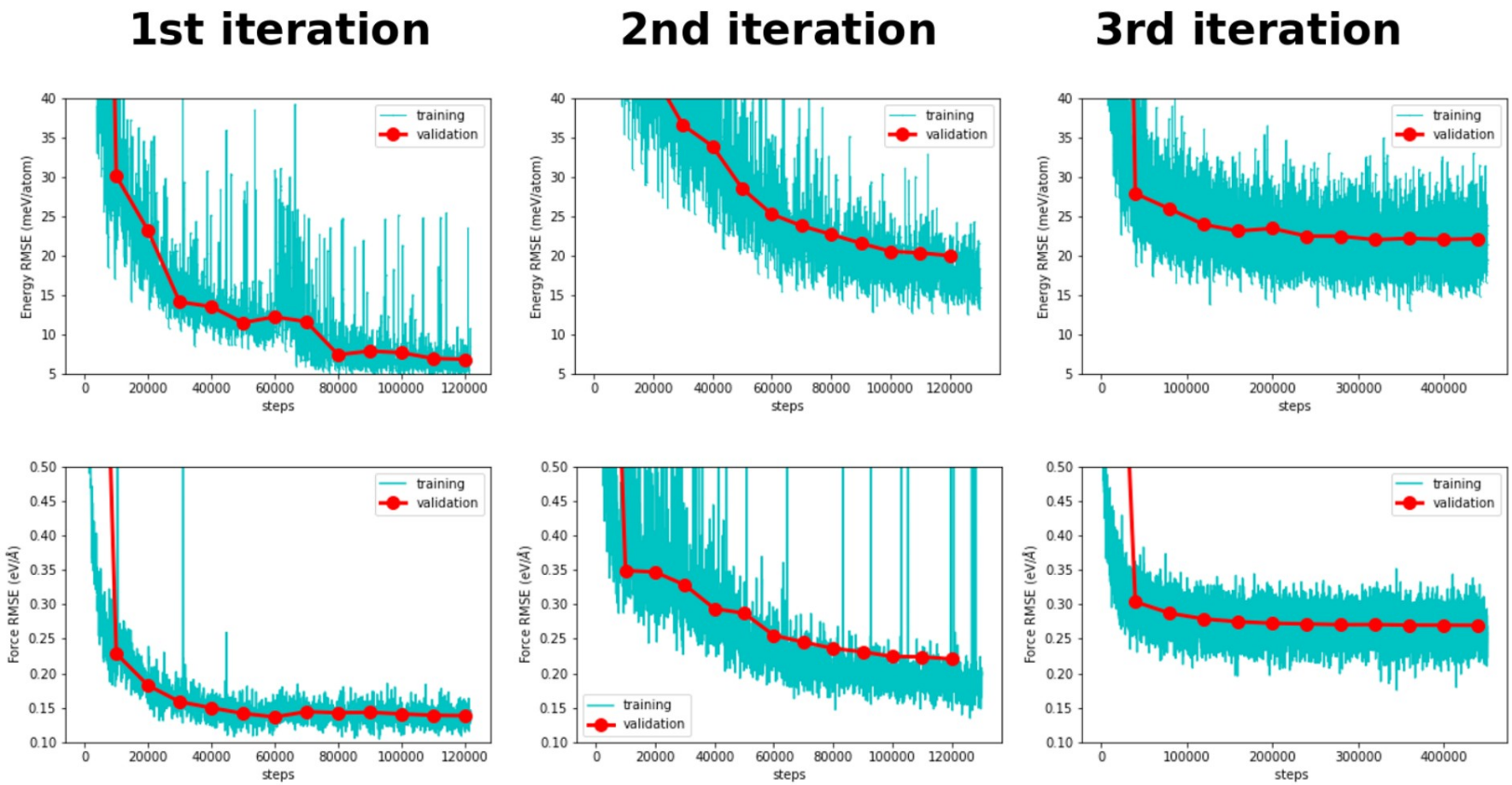

- 20 % of the data set is set aside for validation

Carbon Systems: training and validation

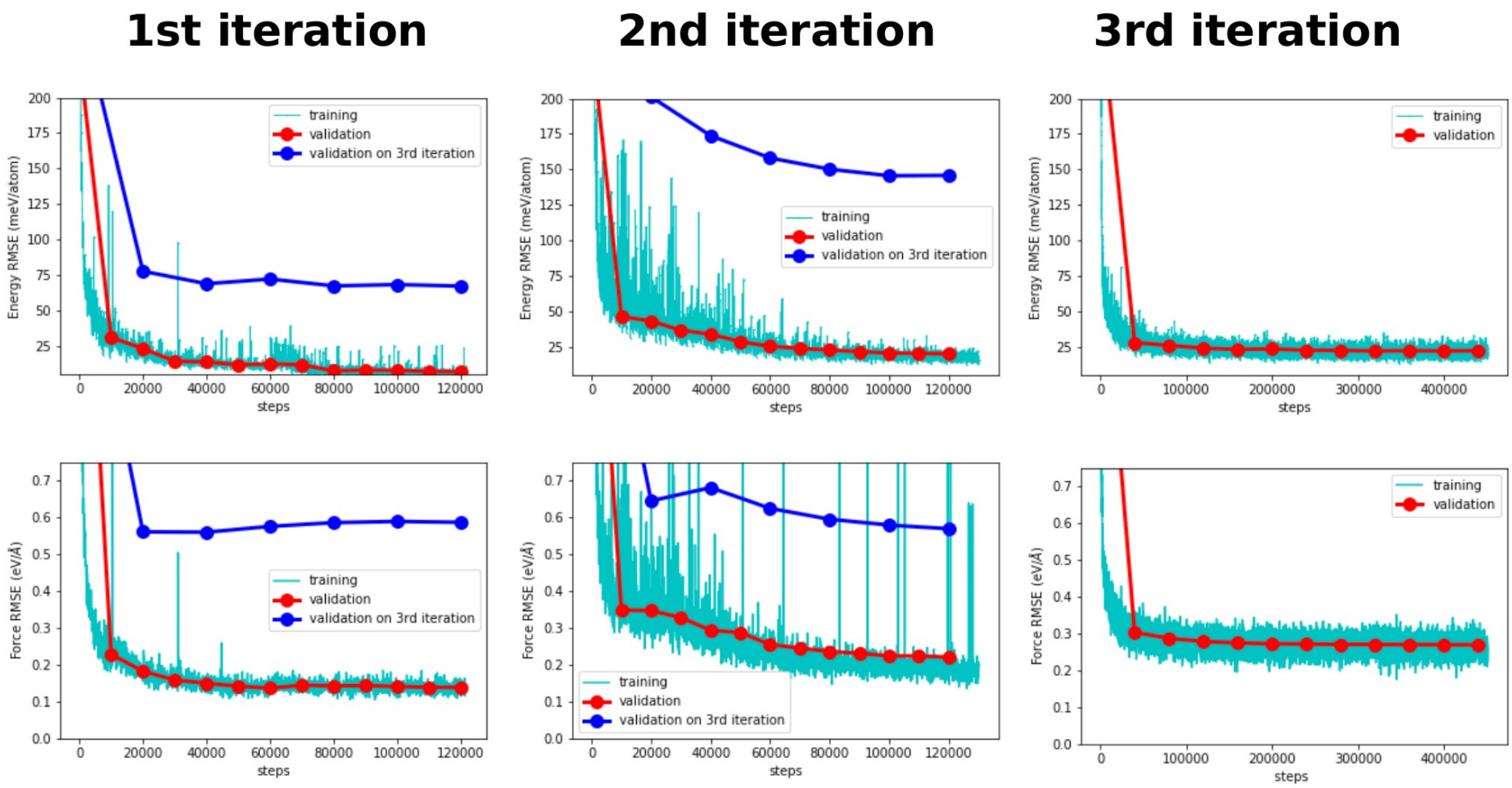

- 20 % of the data set is set aside for validation

Error distribution: energies

1st iteration

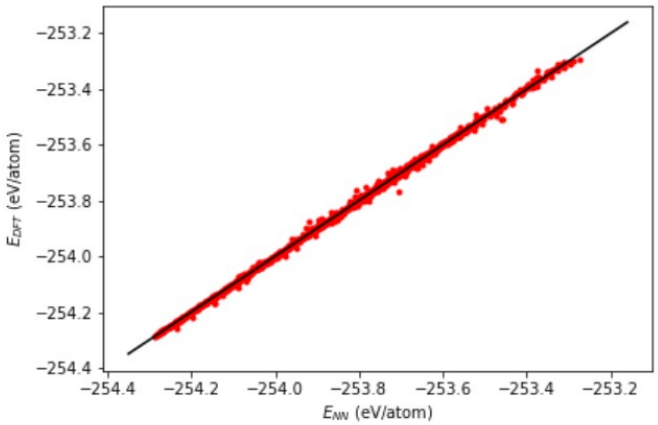

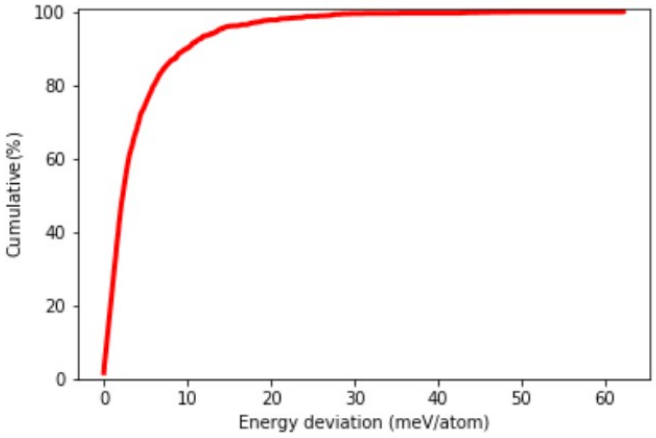

2nd iteration

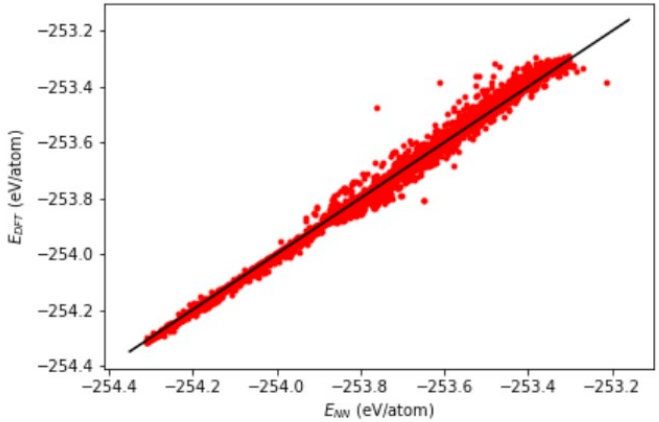

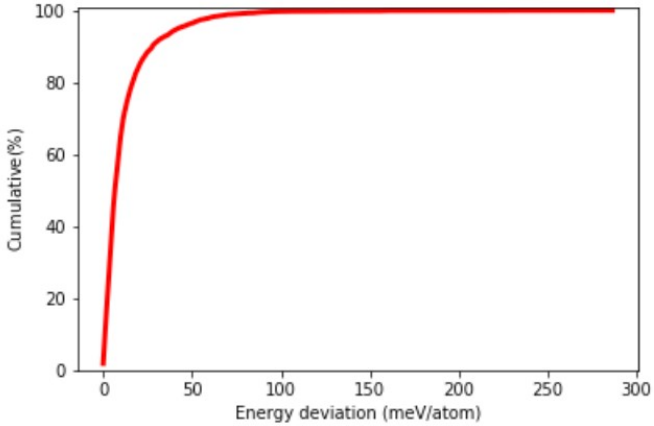

3rd iteration

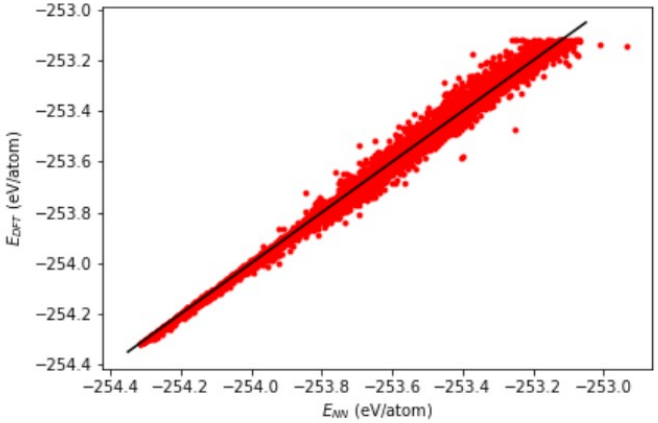

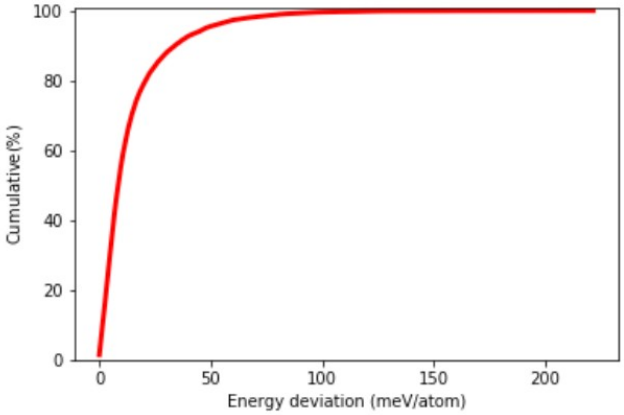

Error distribution: forces

1st iteration

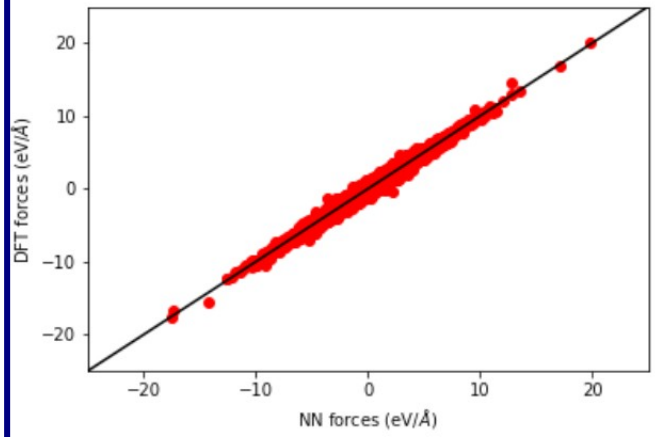

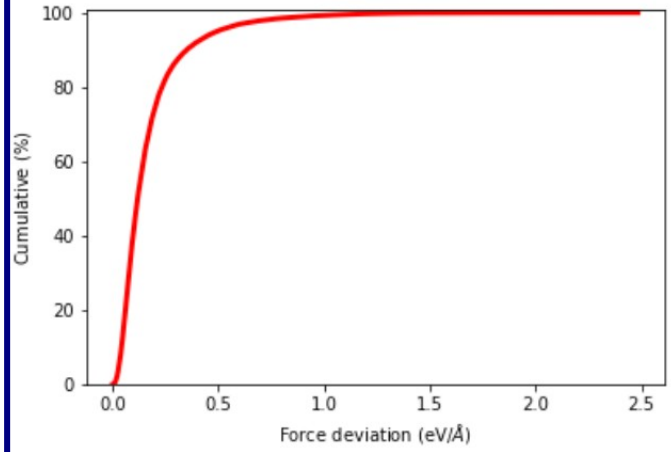

2nd iteration

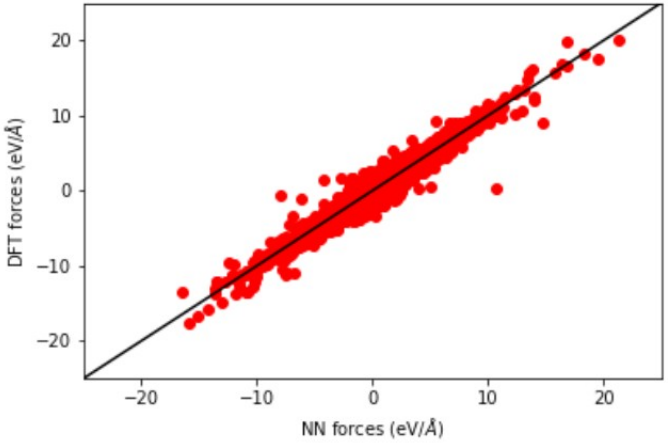

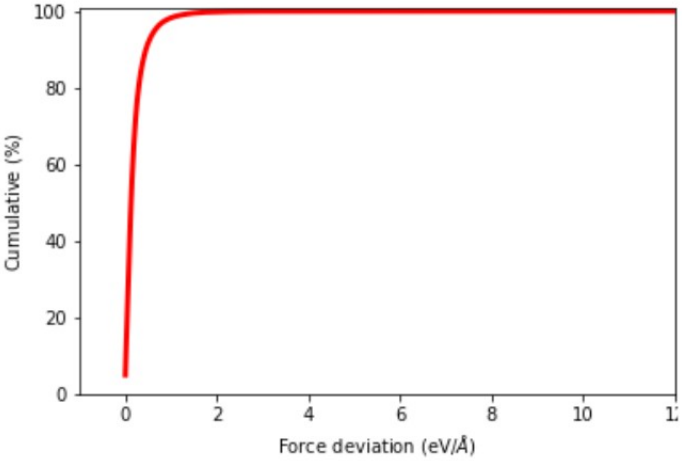

3rd iteration

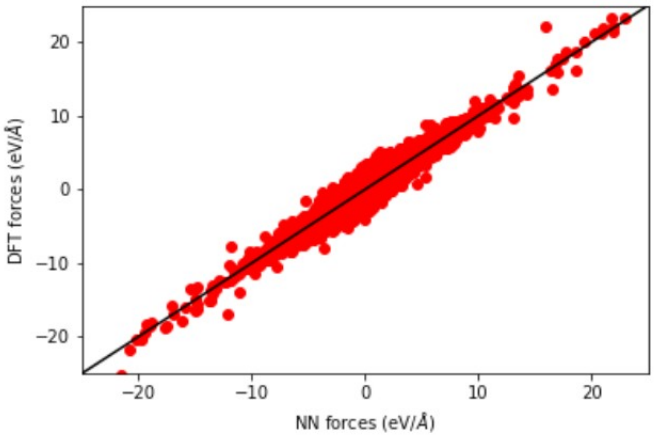

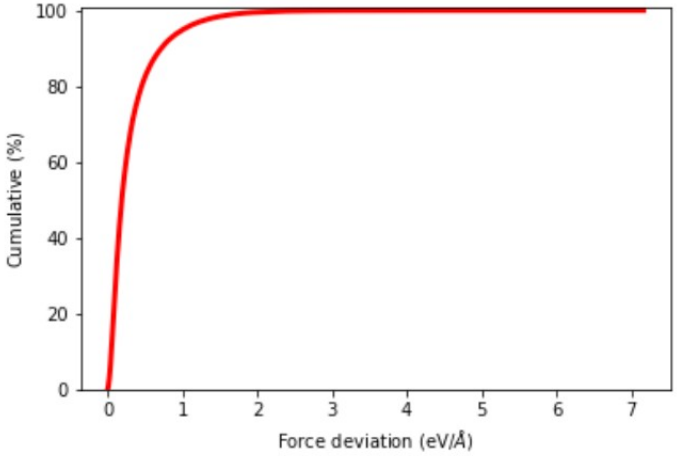

Effect of diversity on training and validation RMSE

Train \ Validate	T error	All D	$D < 0.15$	$D < 0.10$	$D < 0.05$	$D_{12} < 0.05$
All D	22.070	22.131	20.938	15.161	7.659	7.302
$D < 0.15$	18.066	80.424	18.422	13.342	5.949	17.567
$D < 0.10$	8.563	162.327	52.178	9.369	4.391	76.260
$D < 0.05$	2.633	879.207	452.598	89.022	2.585	650.075
$D_{12} < 0.05$	2.574	174.257	88.311	51.972	2.739	2.627

Train \ Validate	All D	$D < 0.15$	$D < 0.10$	$D < 0.05$	$D_{12} < 0.05$
All D	0.2696	0.2717	0.1974	0.0829	0.0785
$D < 0.15$	0.5969	0.2523	0.1789	0.0766	0.1873
$D < 0.15$	0.9571	0.4410	0.1472	0.0617	0.3112
$D < 0.15$	3.2641	2.0028	0.7243	0.0529	0.8699
$D_{12} < 0.05$	0.9641	0.8934	0.5440	0.0529	0.0504

Energy ordering of test structures

- **197 different sp^3 C structures**[3]

Ordering

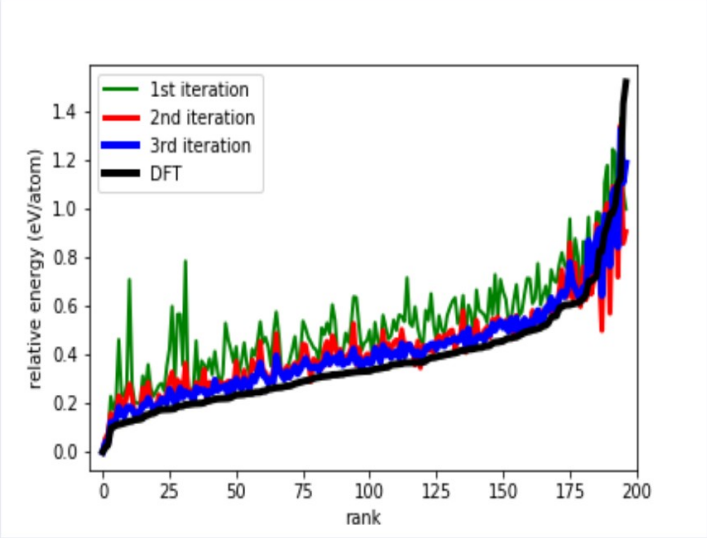

energy correlation

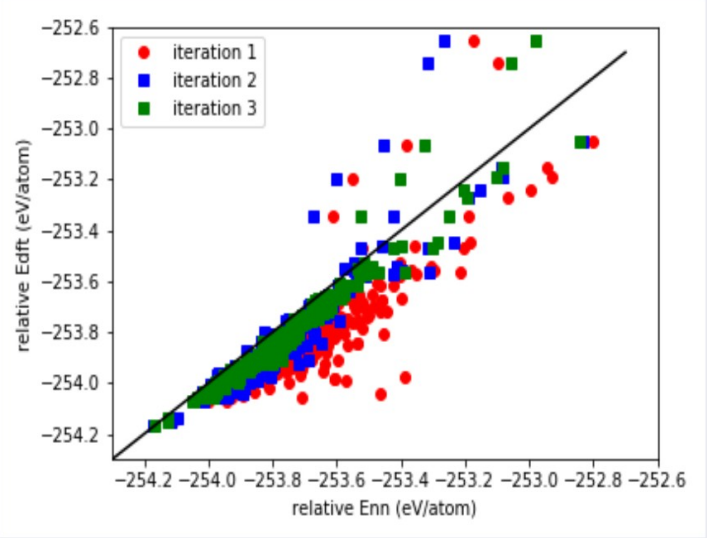

[3] V.L. Deringer, G. Csanyi and D.M.Proserpio, Chem. Phys. Chem. 2017,**18**, 873–877

Energy ordering of test structures

- **197 different sp^3 C structures**[4]

Ordering

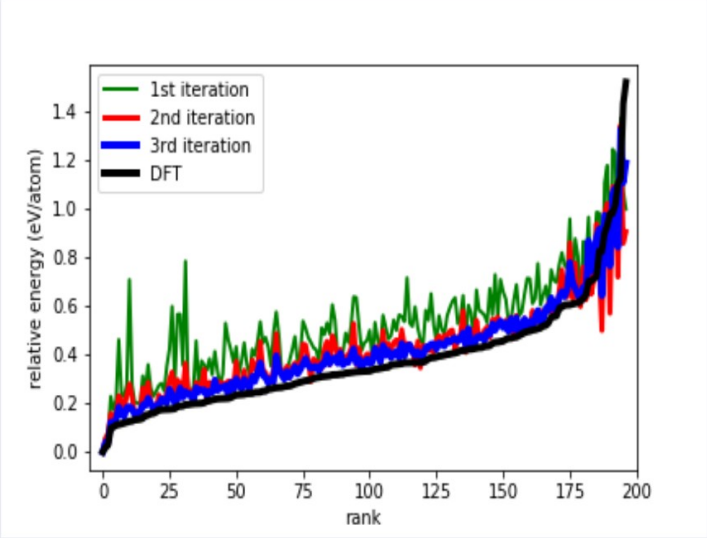

NN vs force fields

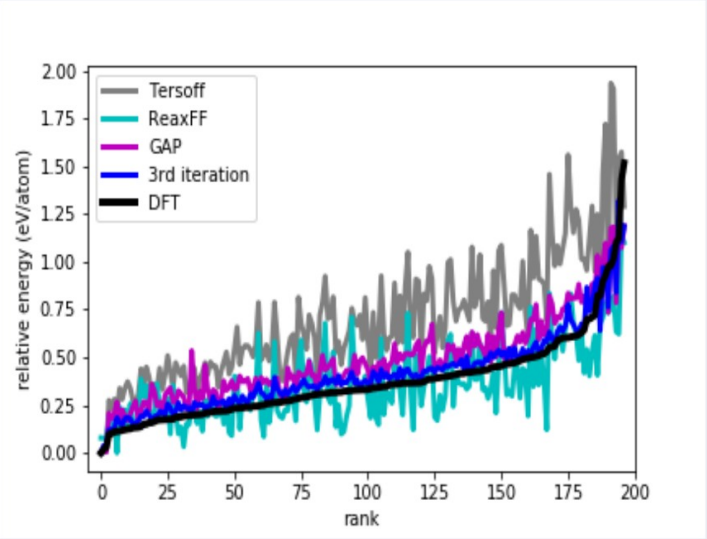

[4] V.L. Deringer, G. Csanyi and D.M.Proserpio, Chem. Phys. Chem. 2017,**18**, 873–877

Equation of State

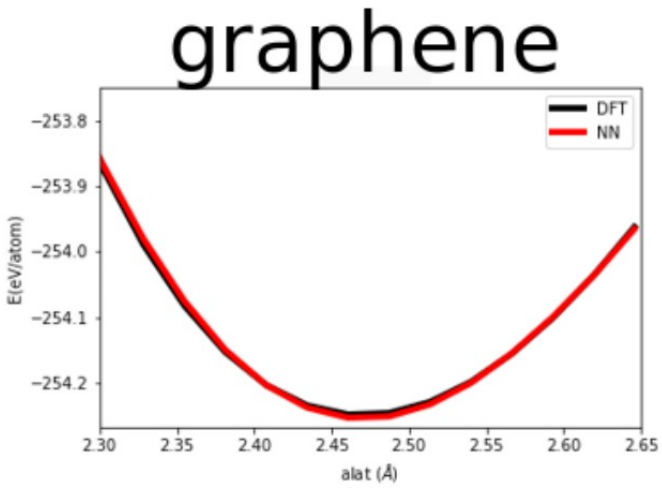

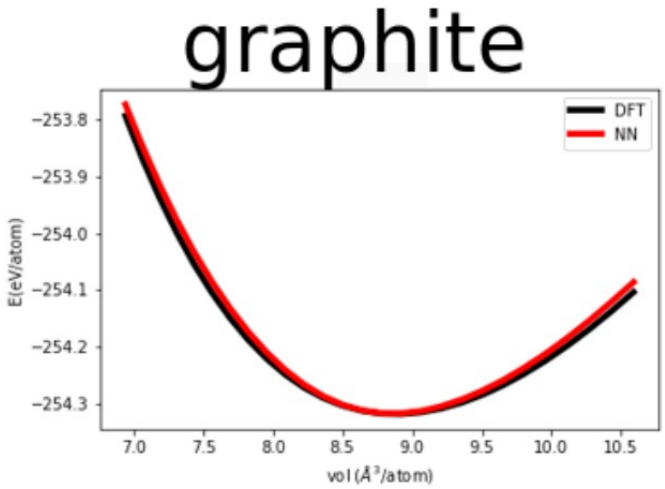

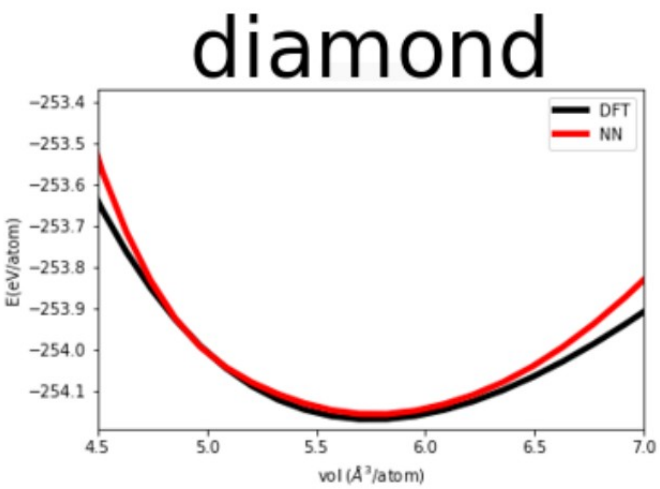

graphene

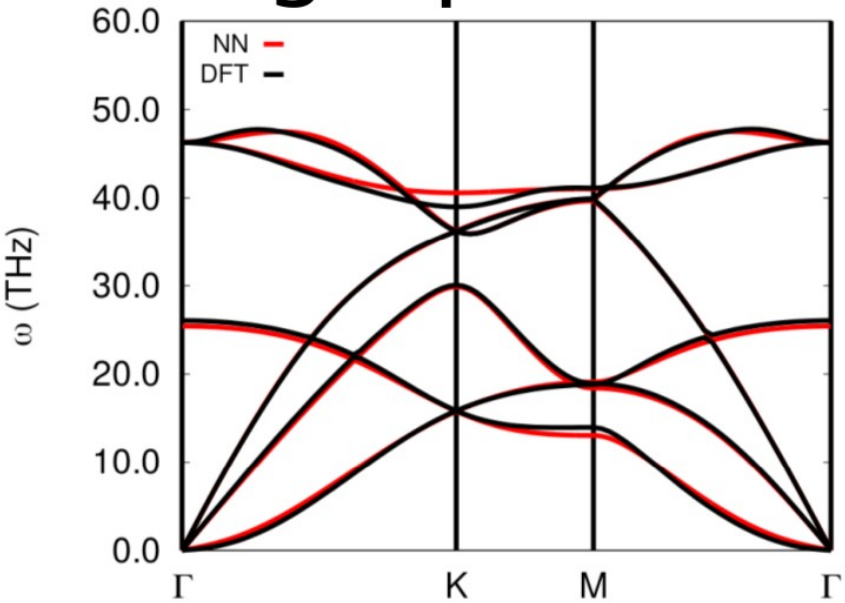

graphite

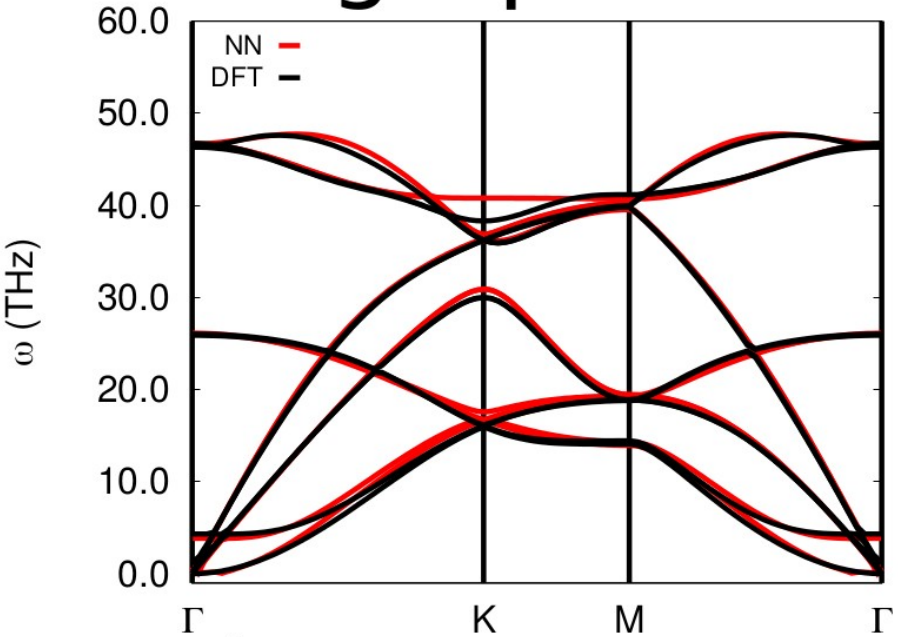

diamond

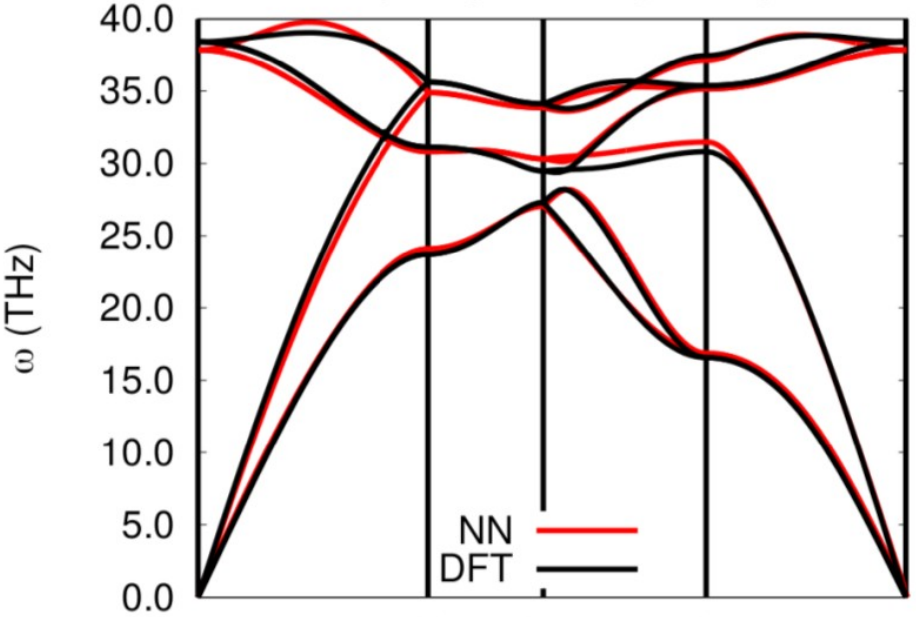

Bilayer Graphene

- configurations generated potential via NVT MD in which the system was heated up from 300 K to 1000K using Nose-Hoover thermostat chain over a period of 1ns.
- Excellent agreement with DFT

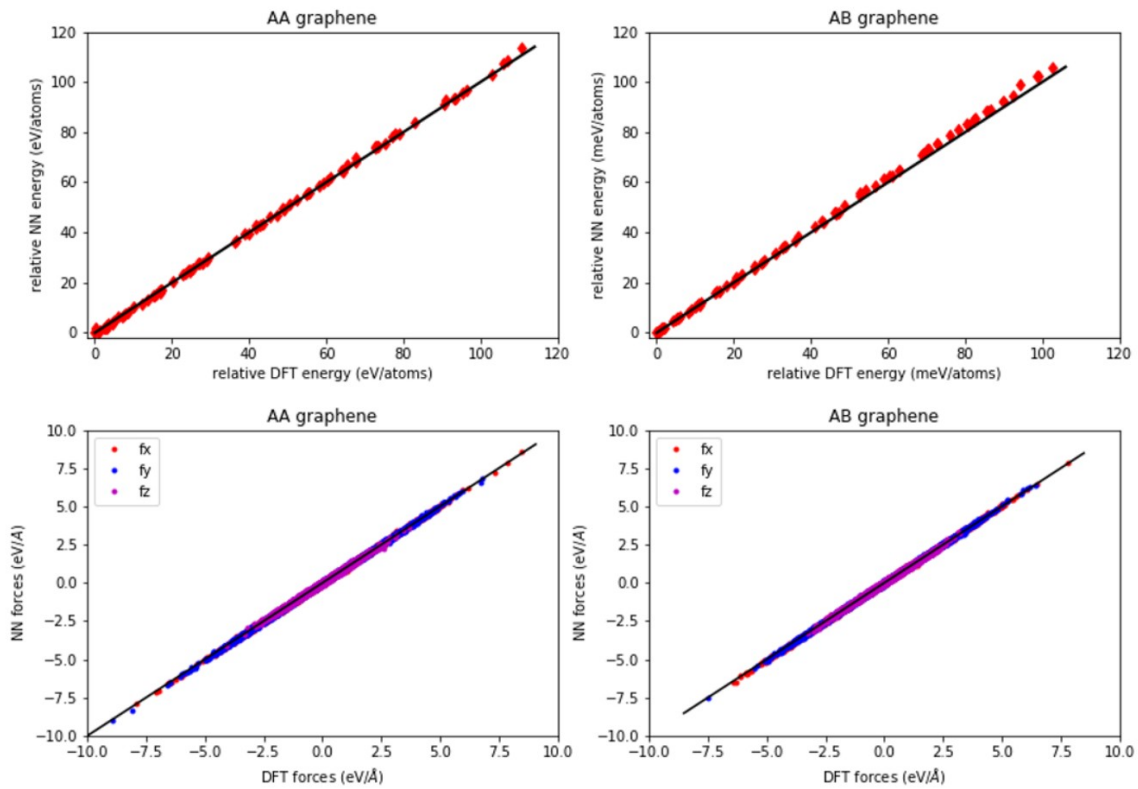

Carbon Nanotubes

- Zigzag nanotube designated by $(n, 0)$ and Armchair nanotube designated by (n, n). n specifies the diameter of the tube as
  $d(n, m) = \frac{a}{\pi}\sqrt{n^2 + nm + m^2}$, a is the lattice parameter
- Trends excellently captured
- Good agreement with DFT

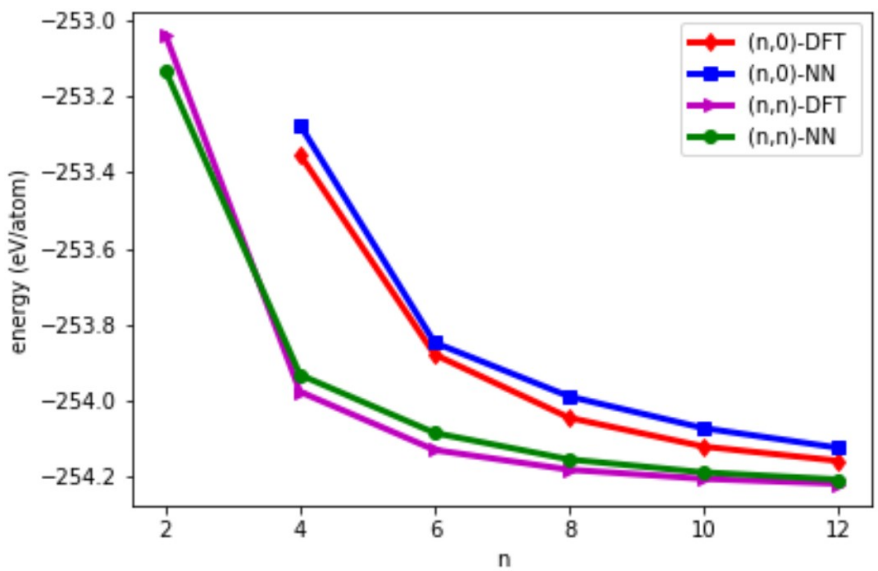

Amorphous Carbon: radial distribution function

a) Our result

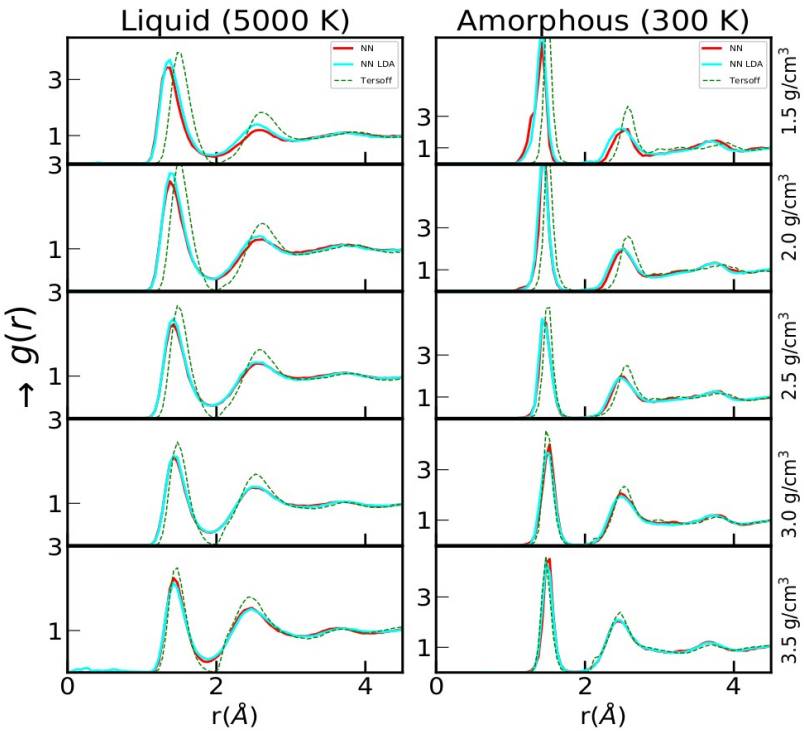

b) GAP

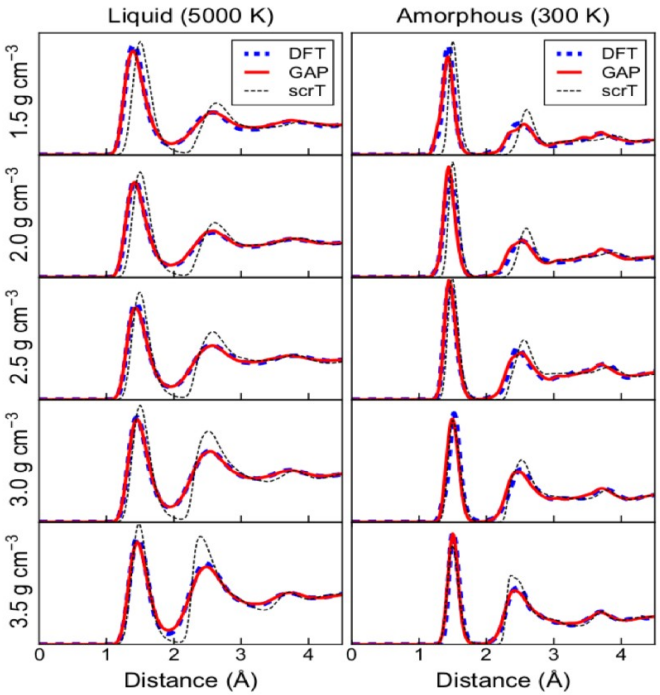

V.L. Deringer and G.Csányi, PRB 95, 094203, (2017)

Amorphous Carbon: sp3 fraction and Young Modulus

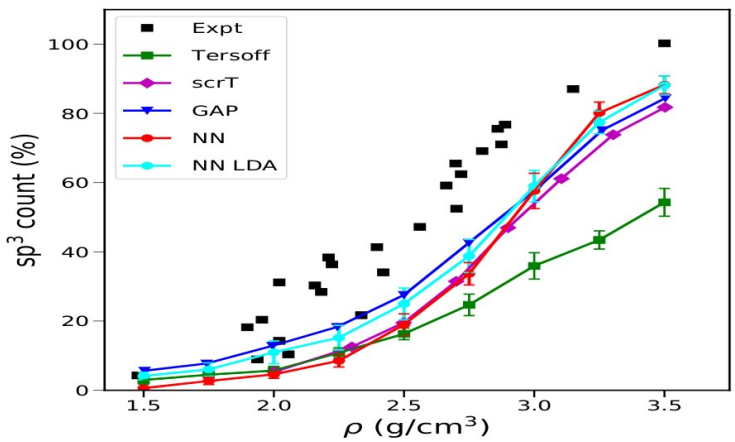

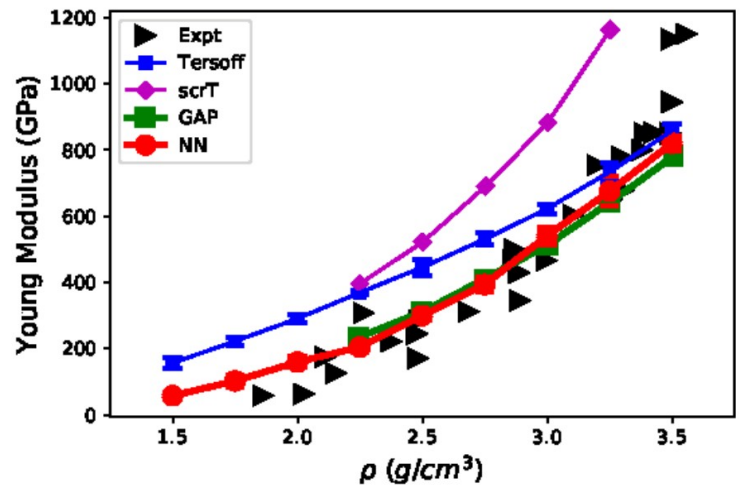

- Fallon et al. PRB 48, 4777 (1993).
- J. Schwan et al. Journal of Applied Physics 79, 1416 (1996)
- V.L. Deringer and G.Csányi, PRB 95, 094203, (2017)
- B.Schultrich et al. Diamond and Related Materials 5 (1996) 914-918
- B.Schultrich et al. Surface and Coatings Technology 98 (1998) 1097-1101

Solid Phase Epitaxy for Silicon

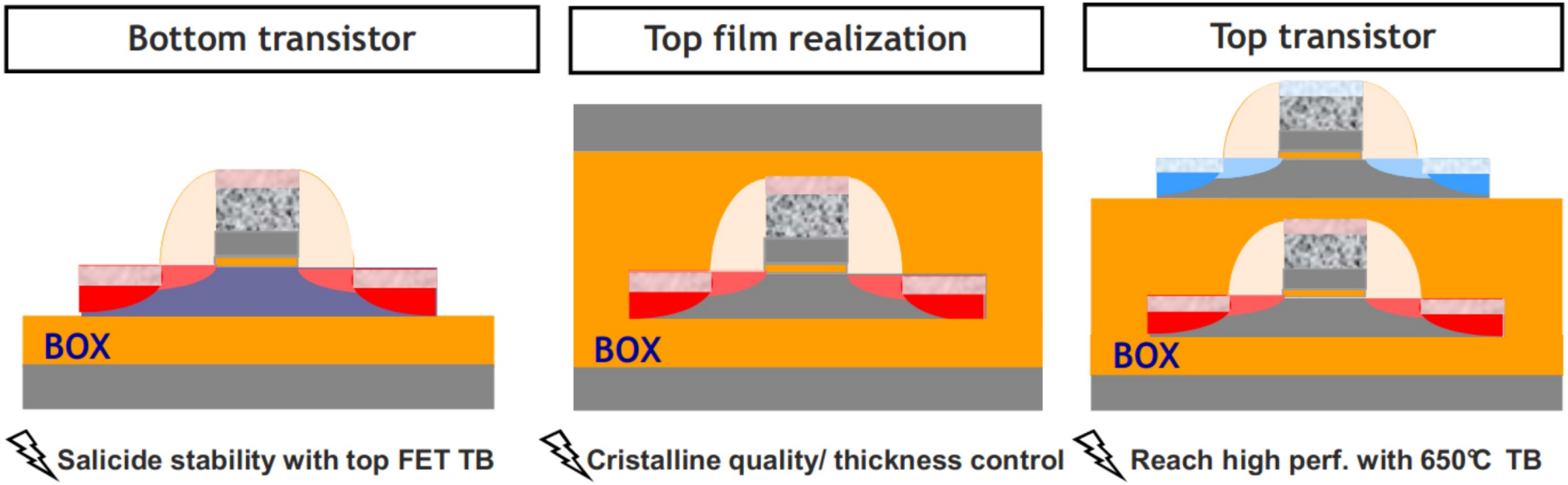

Problem statement

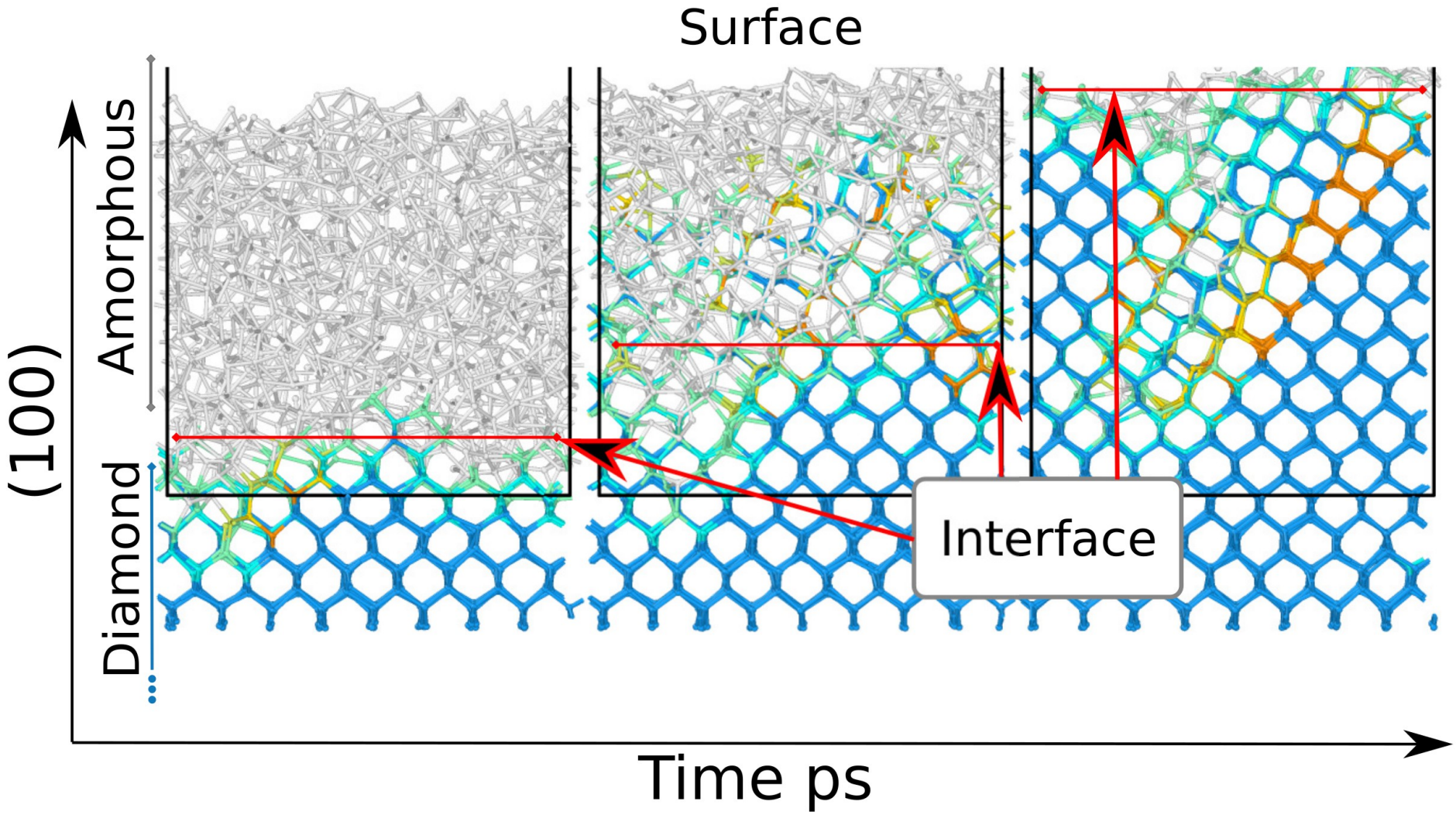

Olson and Roth 1988

The input: $\mathbf{G}_i\left(\{\mathbf{x}_j\}\big|_{d(\mathbf{x}_i,\mathbf{x}_j)<r_{cut}}\right)$

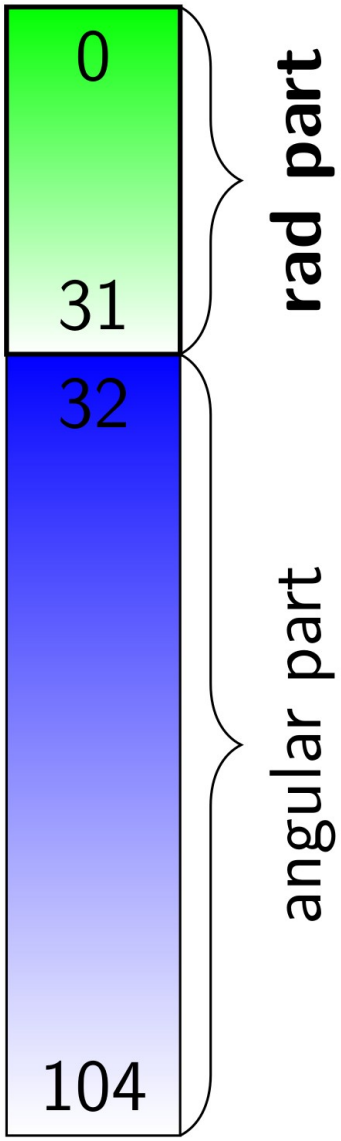

The radial part

$$G^R_{m,s;i} = \sum_{i\neq j}^{\text{All atoms kind s}} e^{-\eta(r_{ij}-R_m)^2} f_c(r_{ij})$$

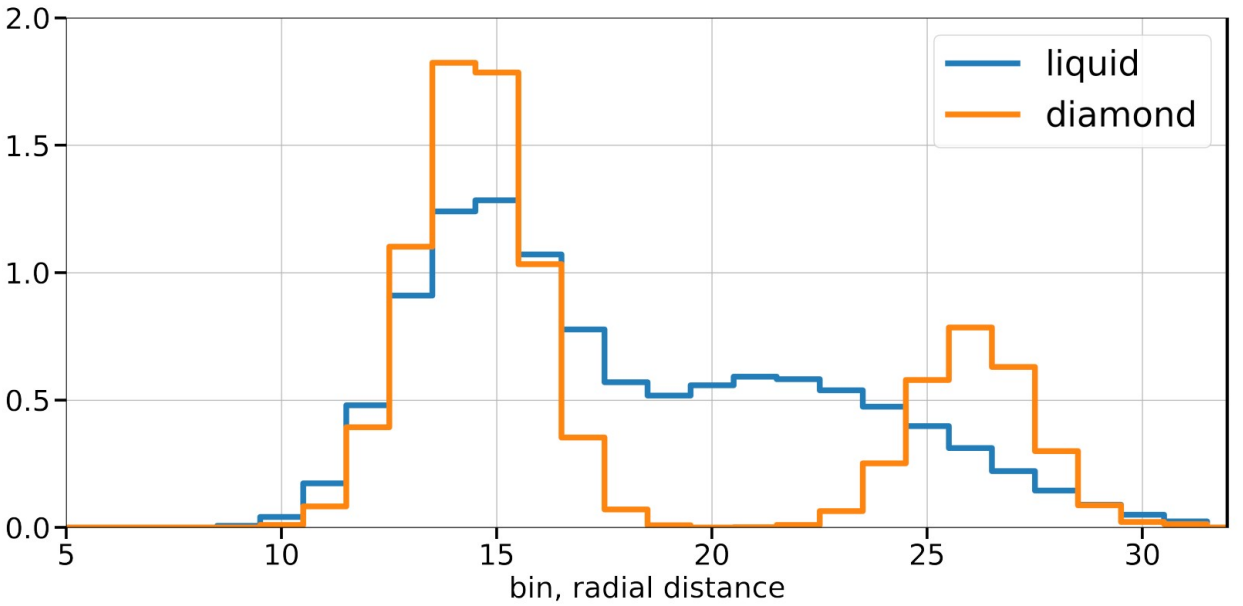

with thermal vibrations

Behler and Parrinello 2007

The input: Descriptor

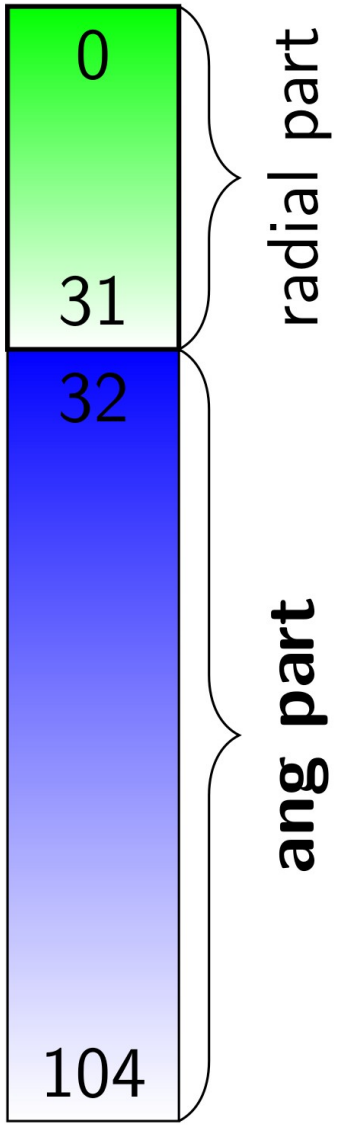

The angular part

$$G^{A}_{n,m,s;i} = 2^{1-\xi} \sum_{j,k \neq i}^{\text{All atom of kind s}} (1 + cos(\Theta_{ijk} - \Theta_n))^{\xi} e^{-\eta\left(\frac{r_{ij}+r_{ik}}{2} - R_m\right)^2} f_c(r_{ij}) f_c(r_{ik})$$

Lot et al. 2020; Smith, Isayev, and Roitberg 2017

From a FFNN to a potential

Structure

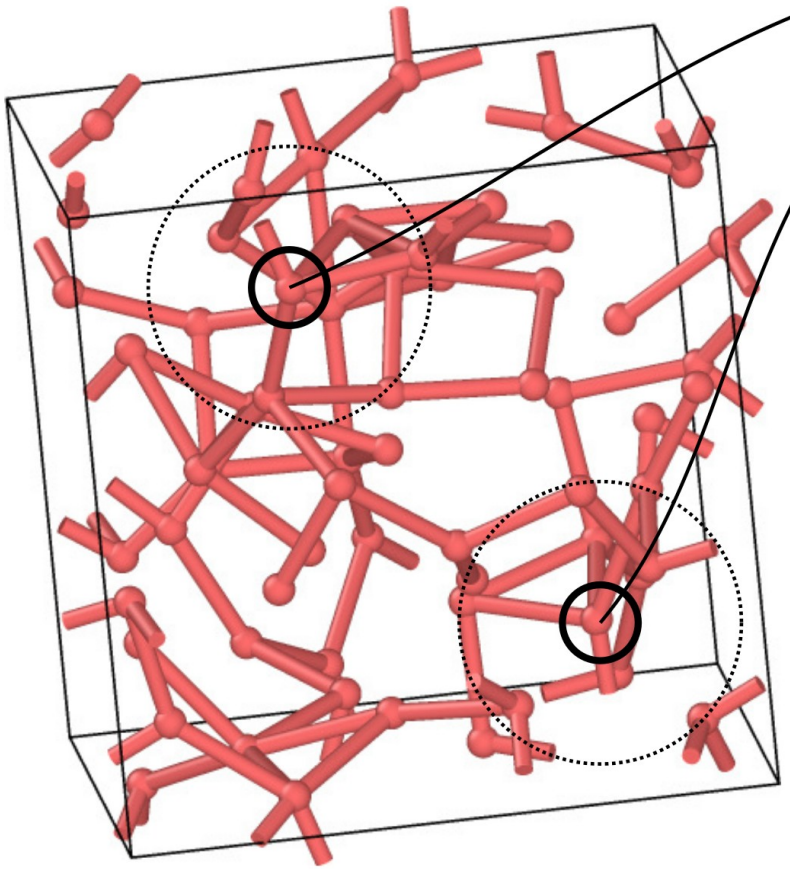

$$G\left(\{\mathbf{r}_i | r_i - r < r_c\}\right)$$

Features vectors

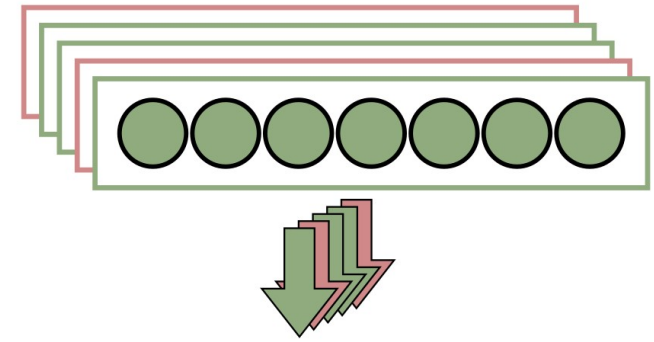

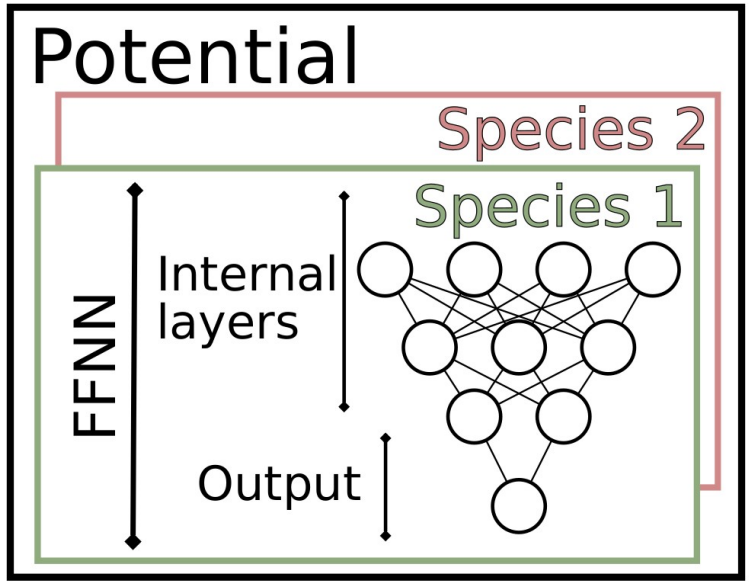

Total energy: $E = \sum_i E_i$

The fitting phase

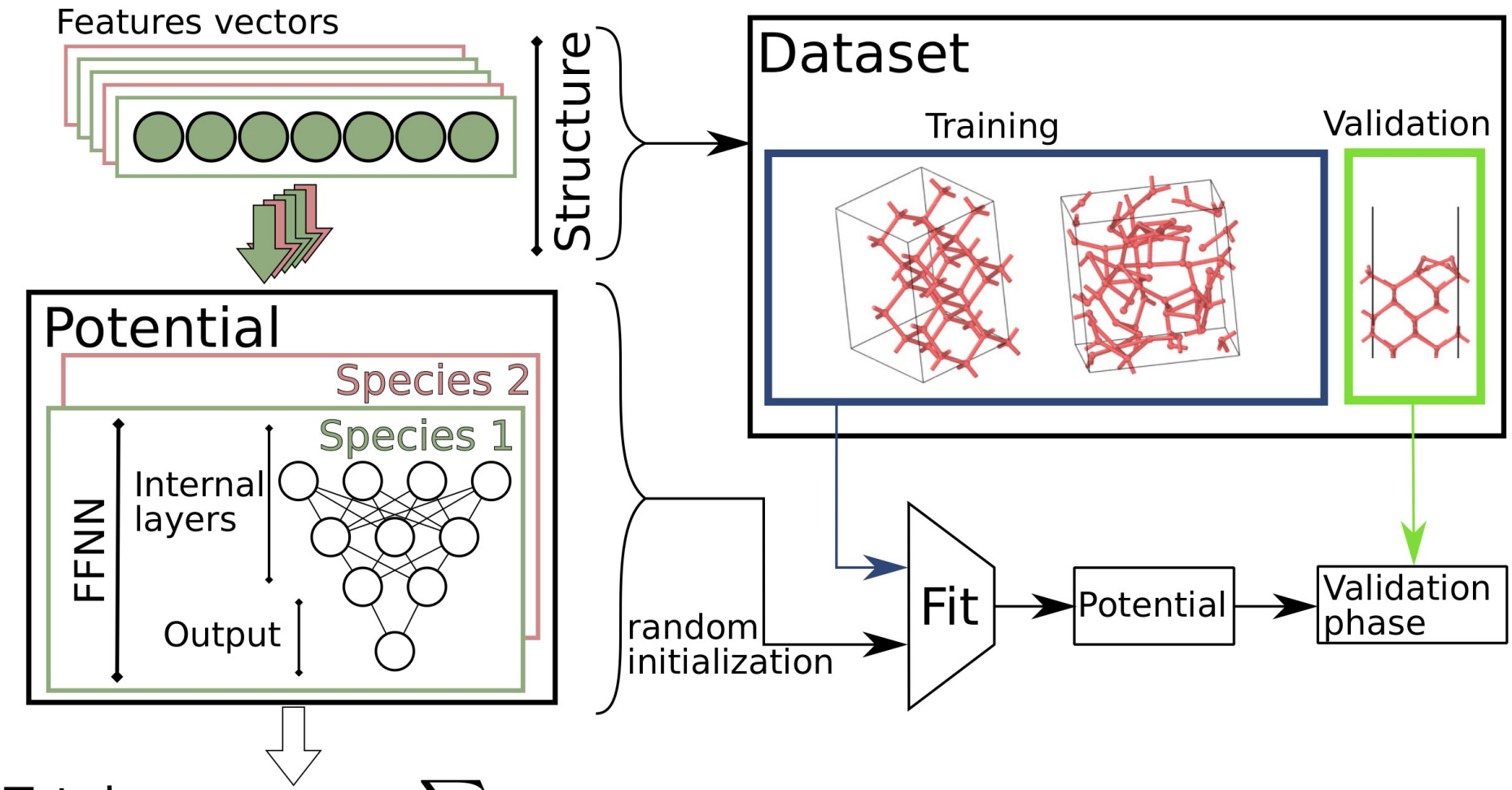

Total energy: $E = \sum_i E_i$

Work workflow

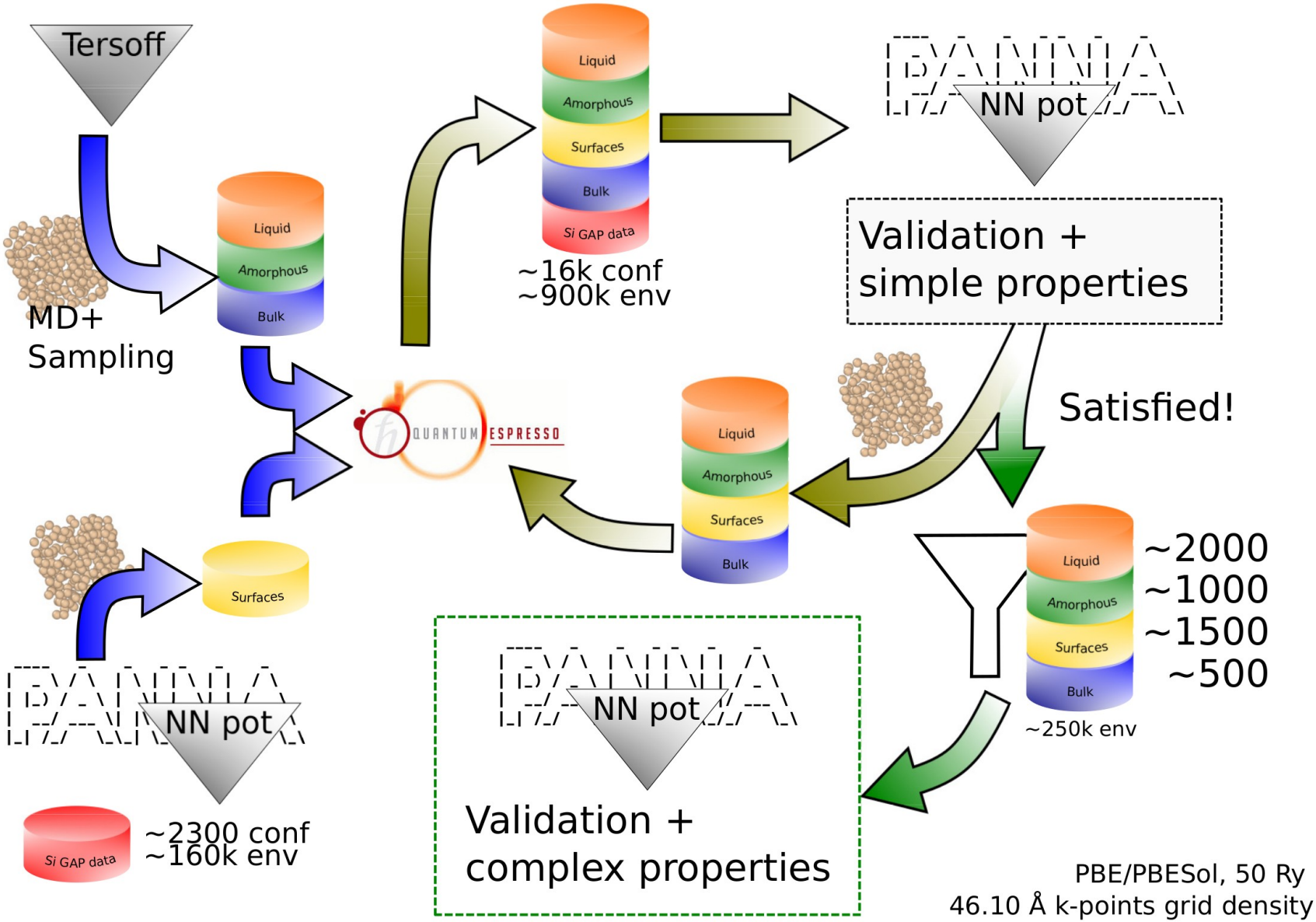

Shaidu et al. 2021; Artrith and Urban 2016; Bartók et al. 2018

Dataset and validation

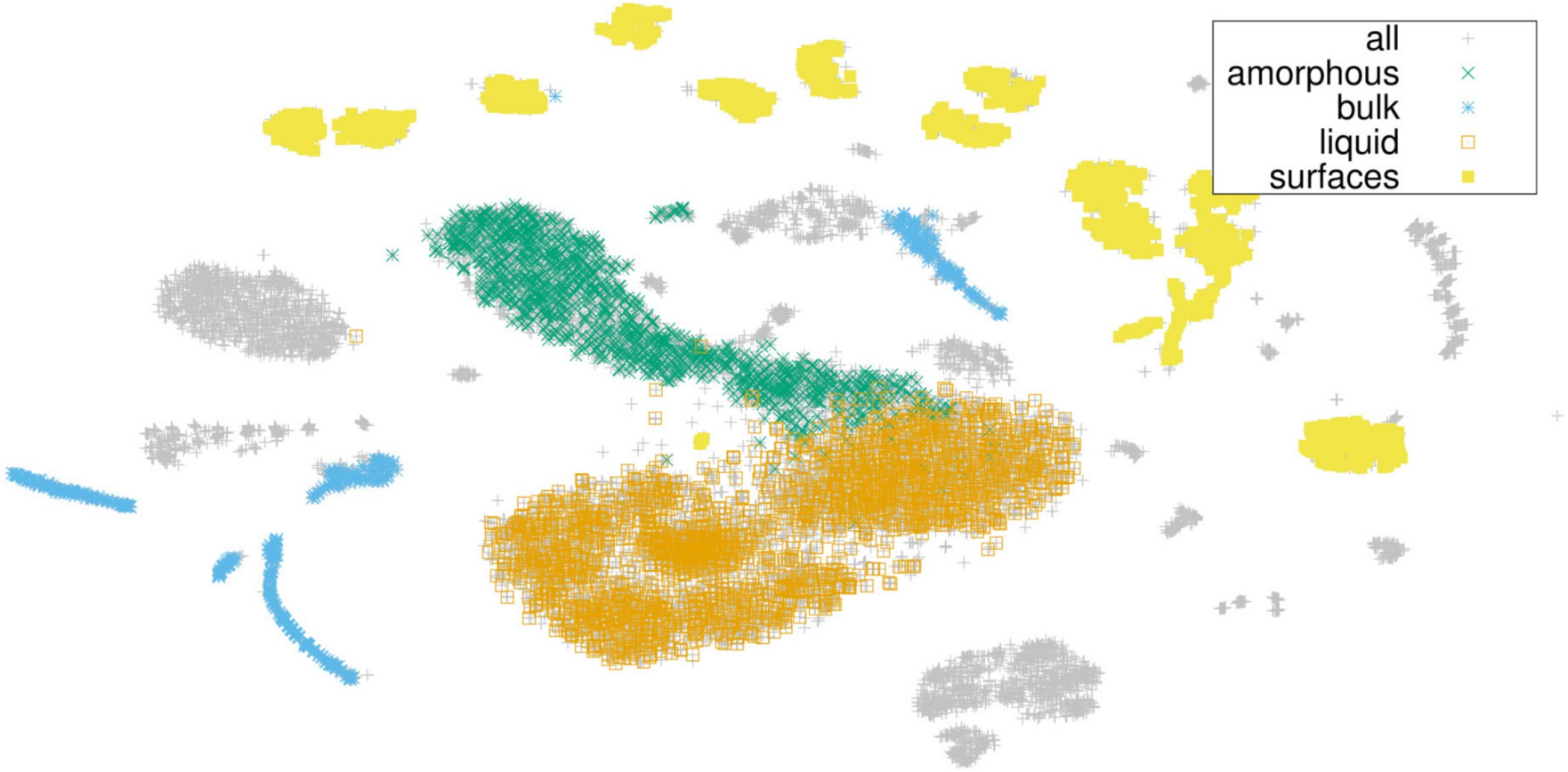

t-sne, $\approx$ 5000 points for $\approx$ 250k environments

Validation on the dataset

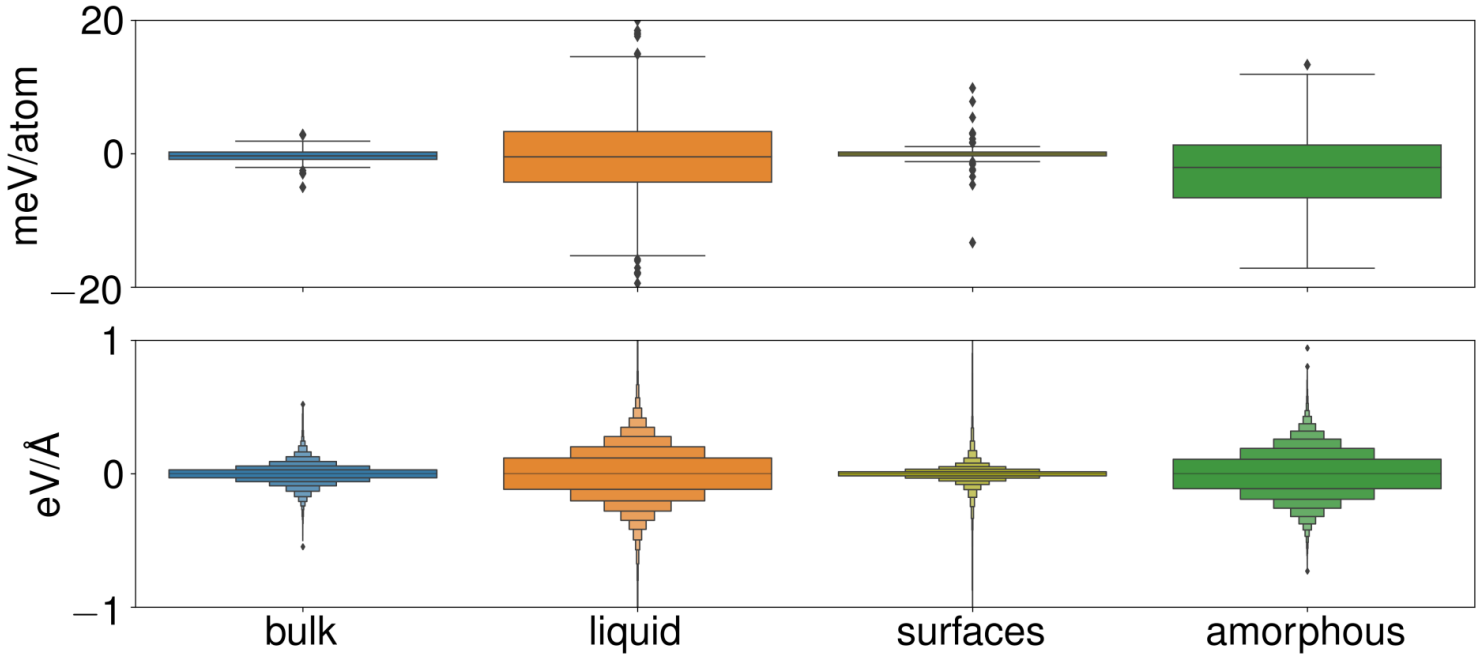

	bulk	liquid	surfaces	amorphous
Energy [meV/atom]	0.9	7.5	3.4	5.8
Forces [meV/Å]	66	196	103	170

Validation on physical properties

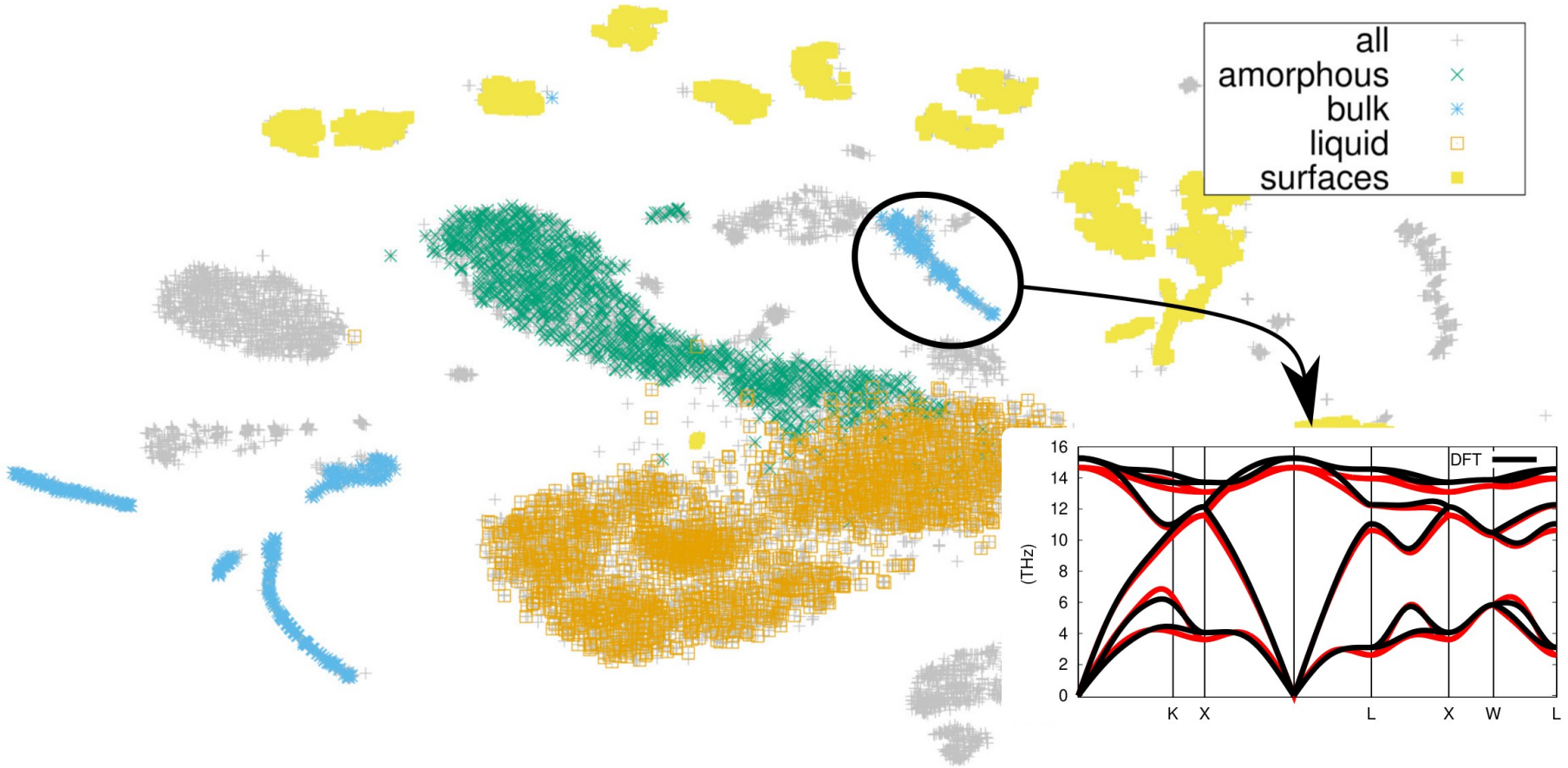

Validation on physical properties

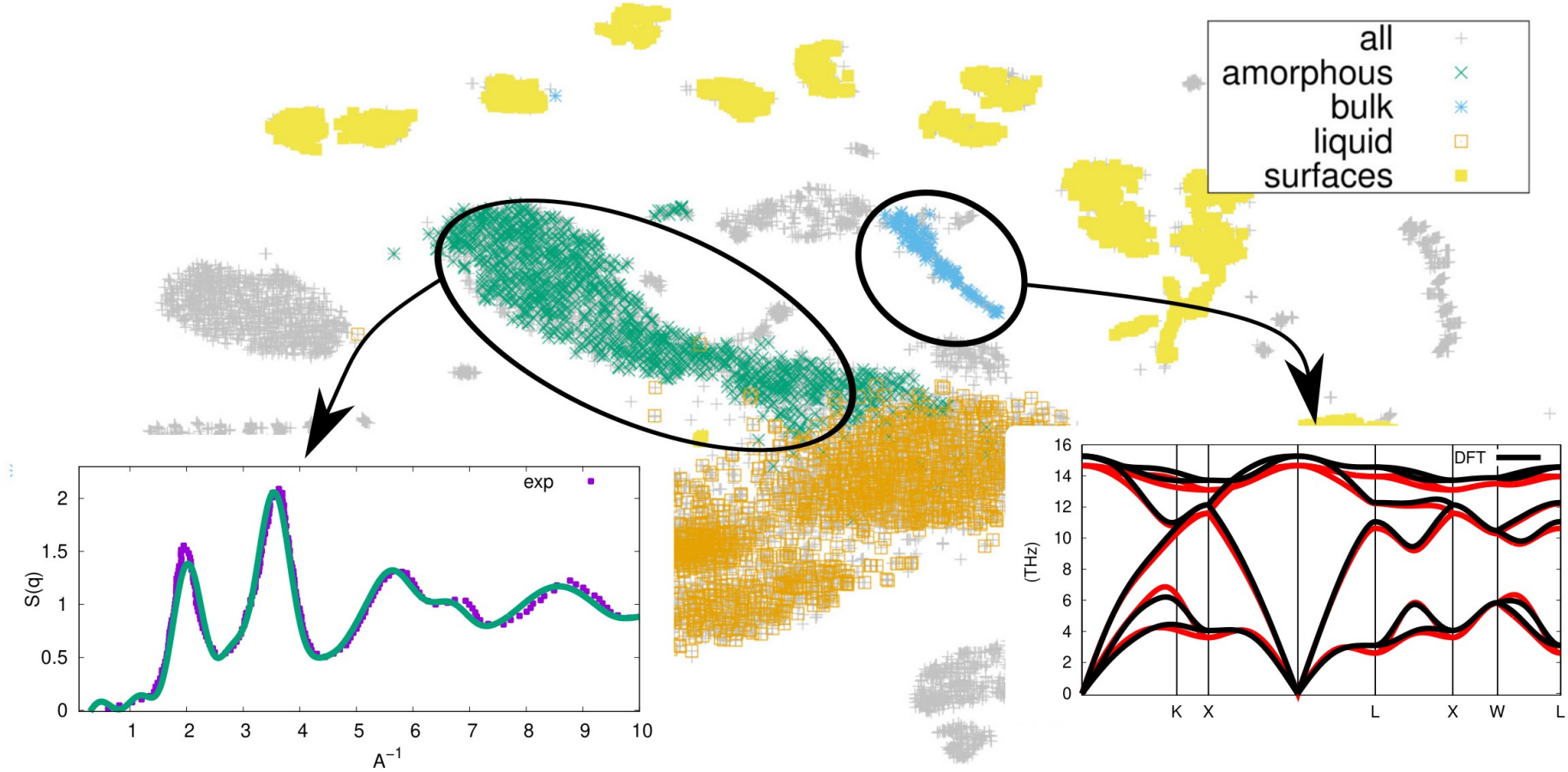

Validation on physical properties

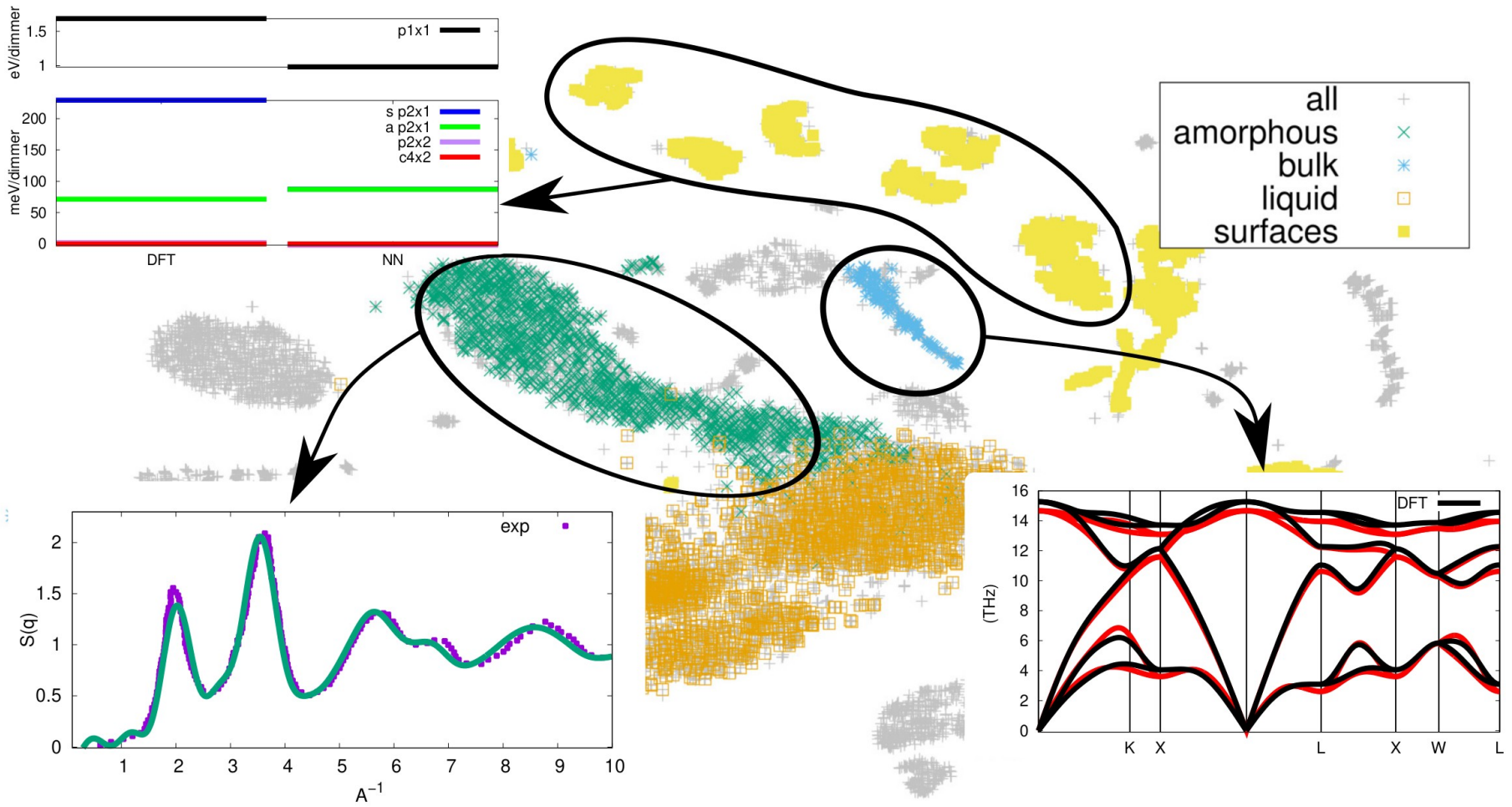

Validation on physical properties

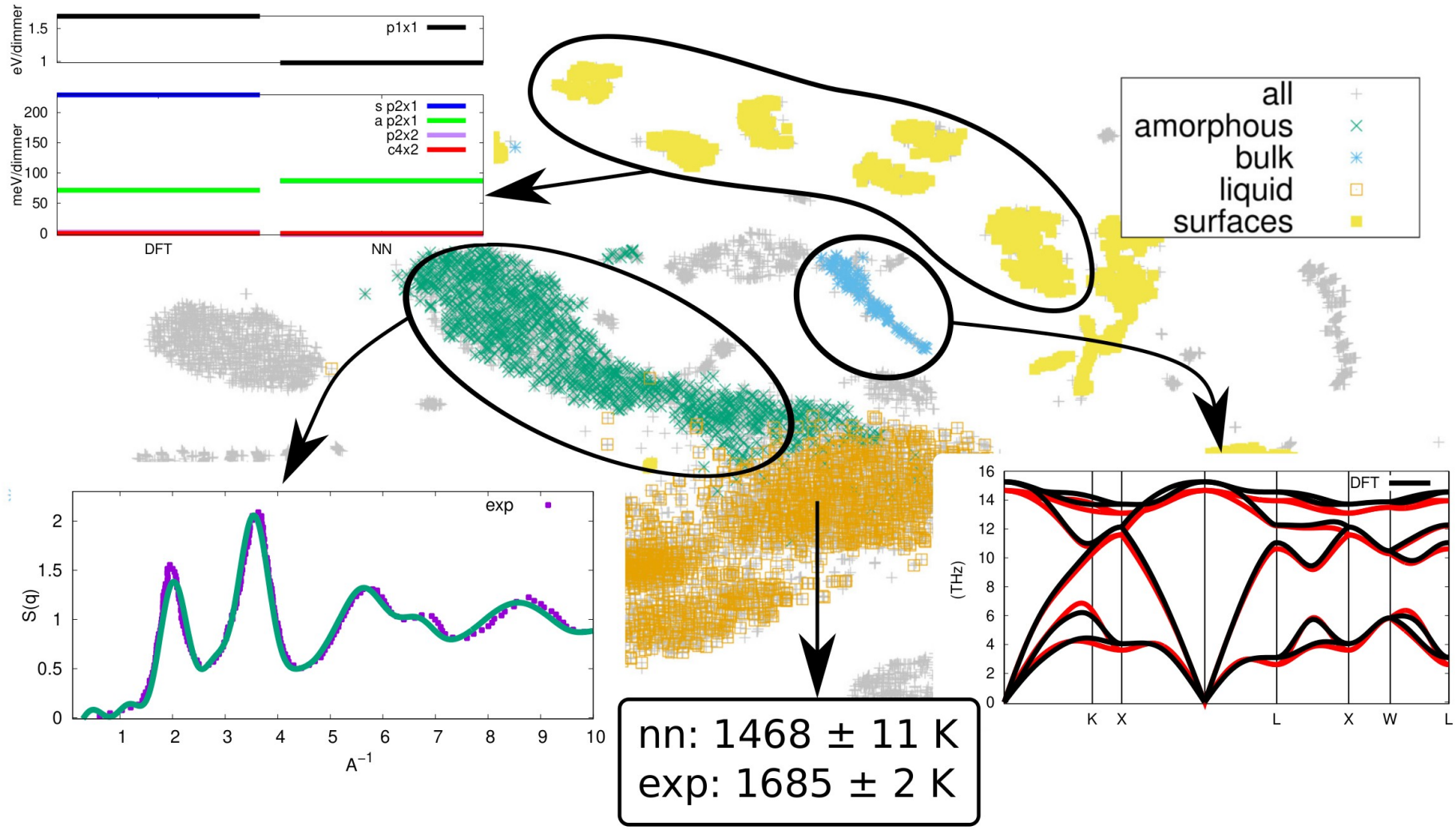

Melting temperature

NN pbe	1468 ± 11K
DFT pbe	1540 ± 50K
NN PBESol	1194 ± 28K
GAP PBESol	1213 ± 21K
Experiments	1685 ± 2K

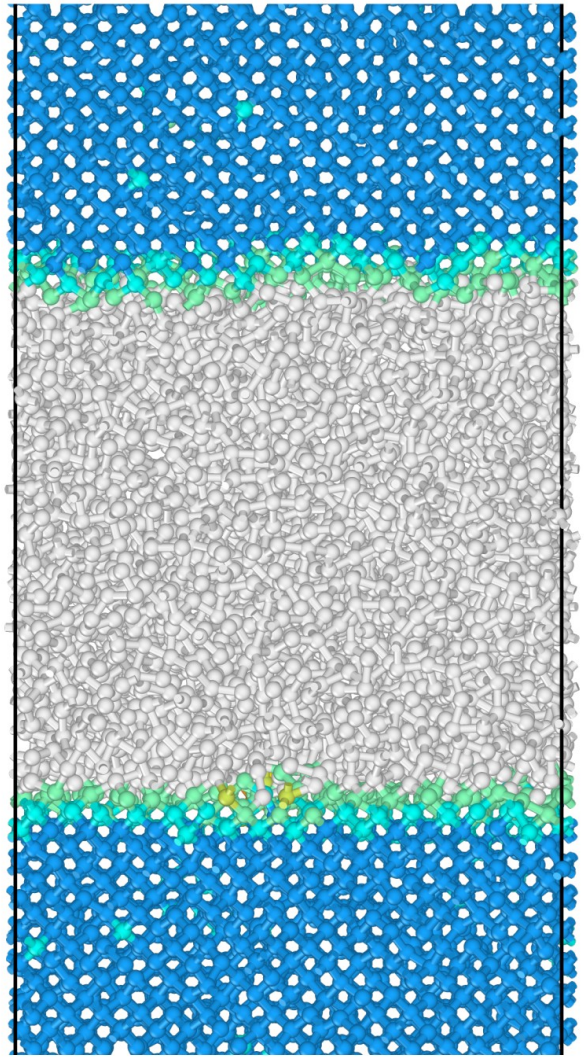

Yoo, Xantheas, and Zeng 2009; Jinnouchi, Karsai, and Kresse 2019

SPE, What do we see?

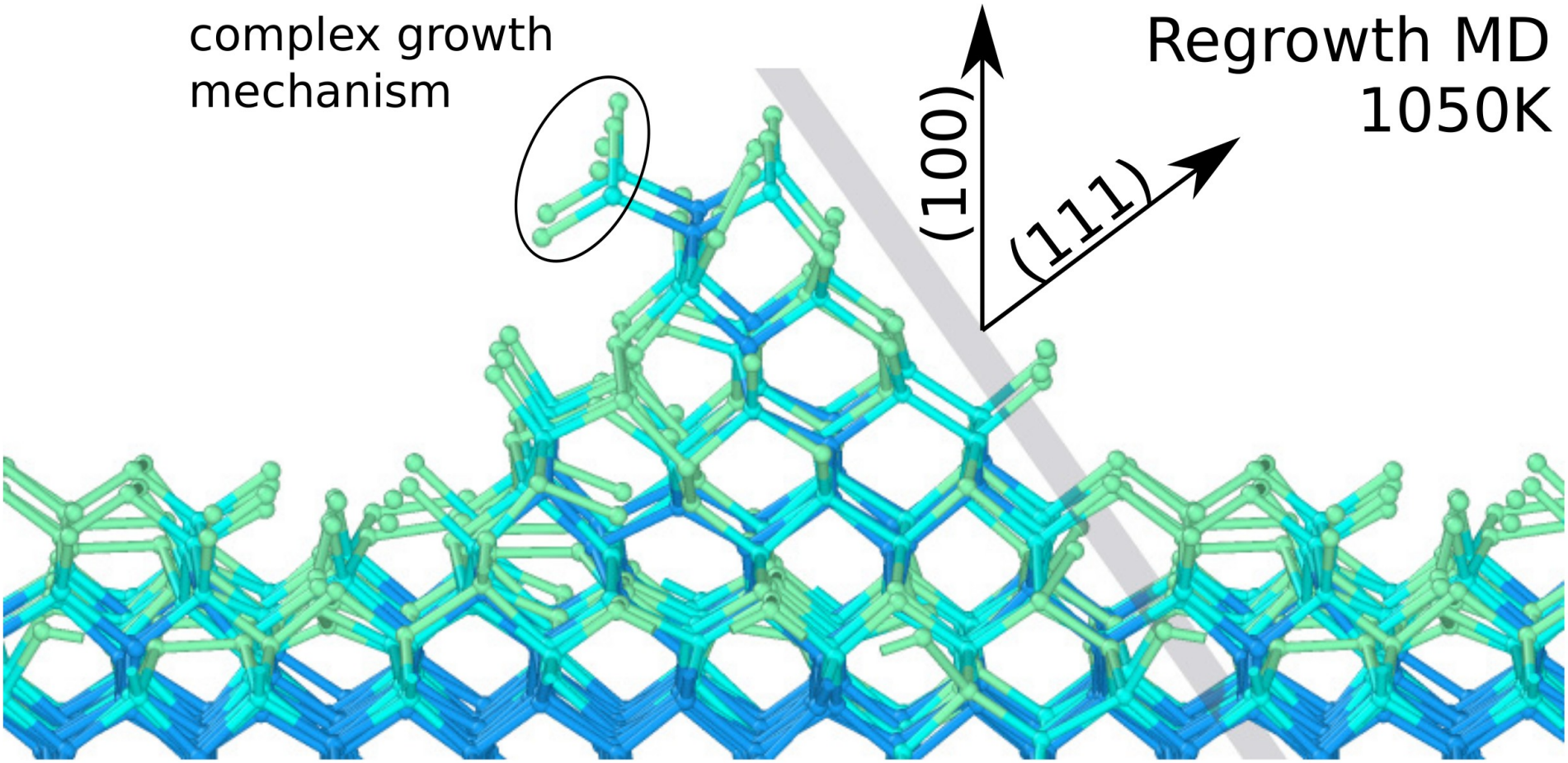

Thermally activated process:

$$v = v_0 exp(-\frac{\Delta E}{k_b T})$$

SPE, What do we see?

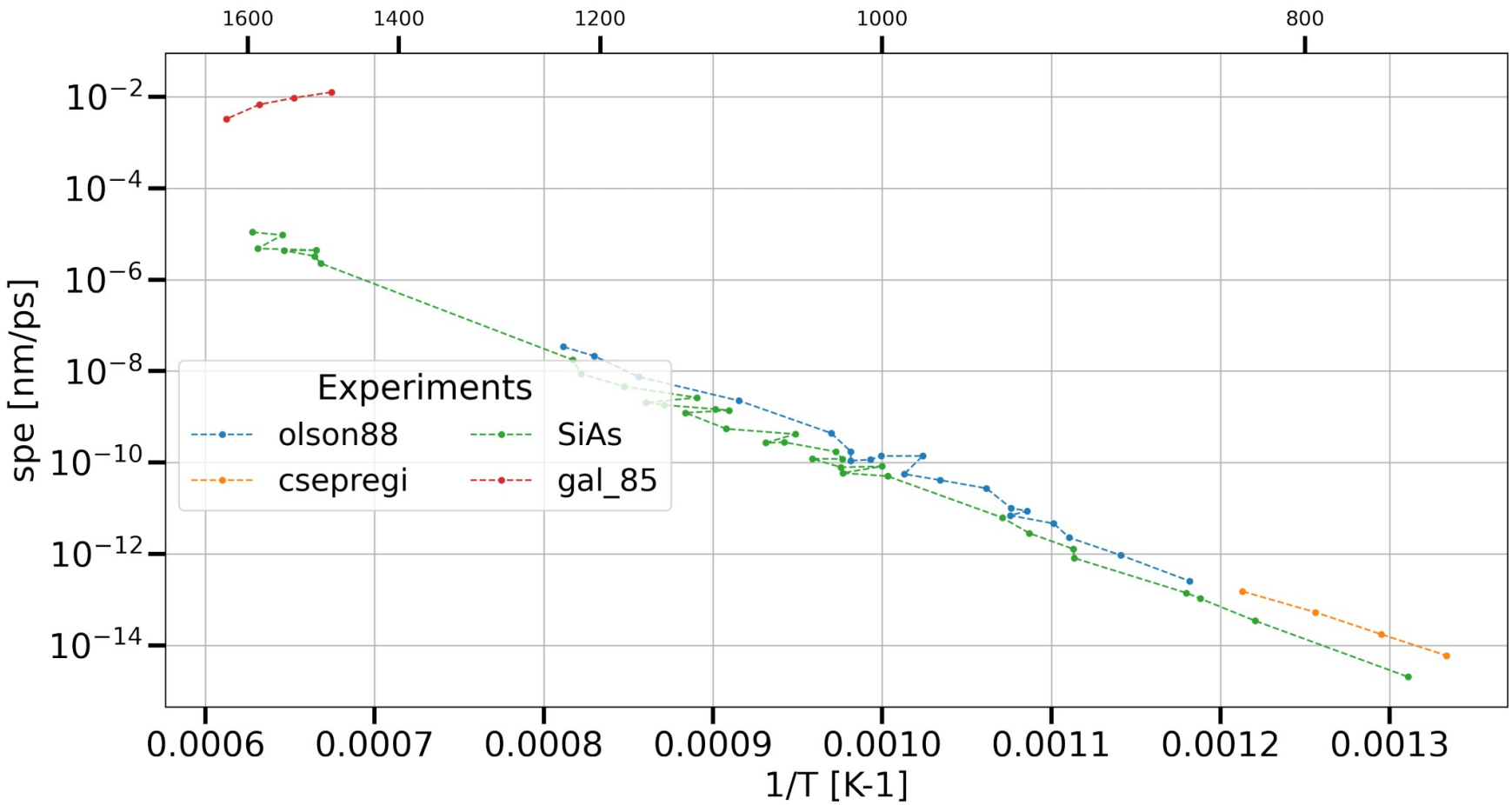

SPE, What do we see?

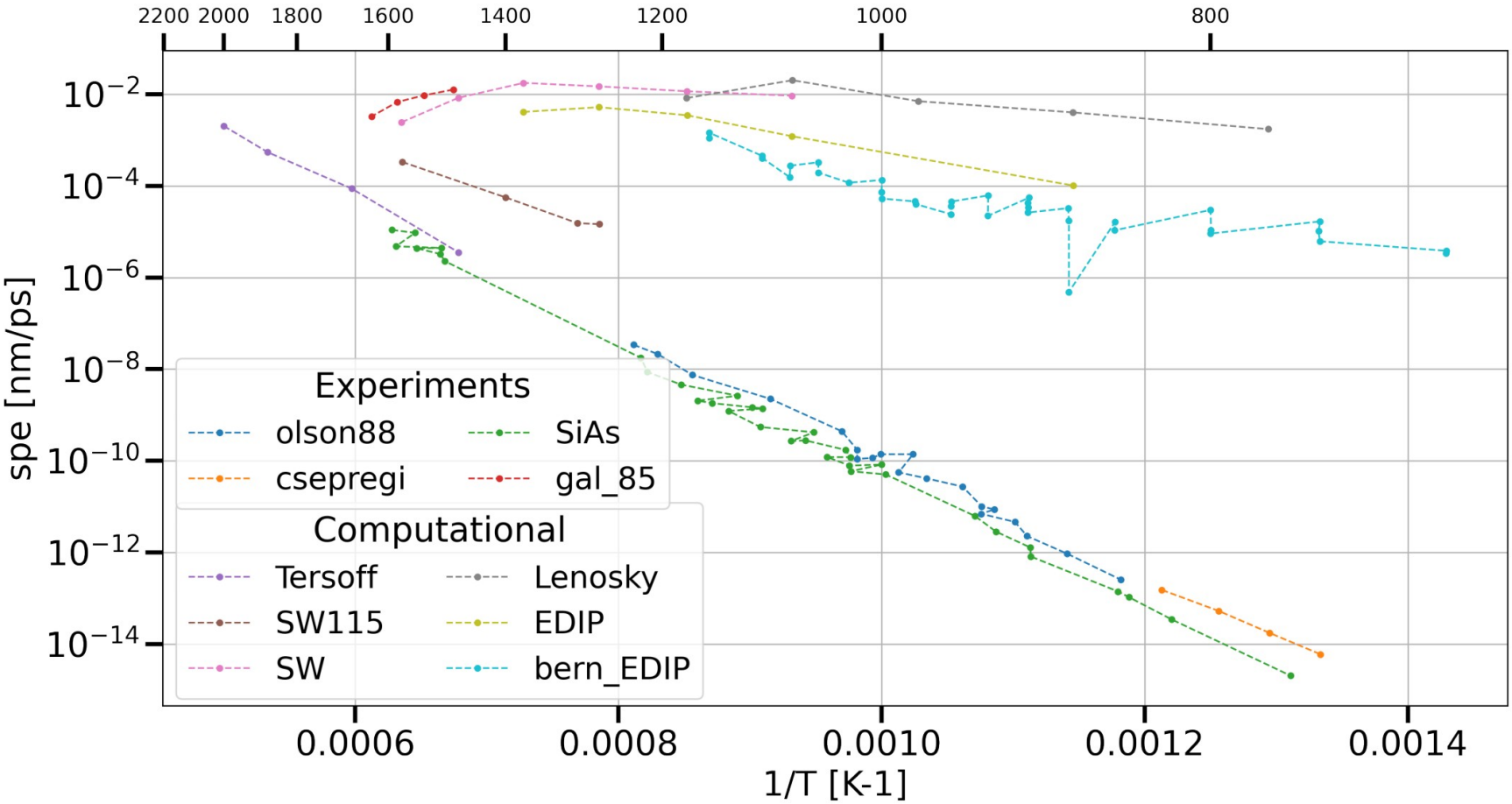

SPE, What do we see?

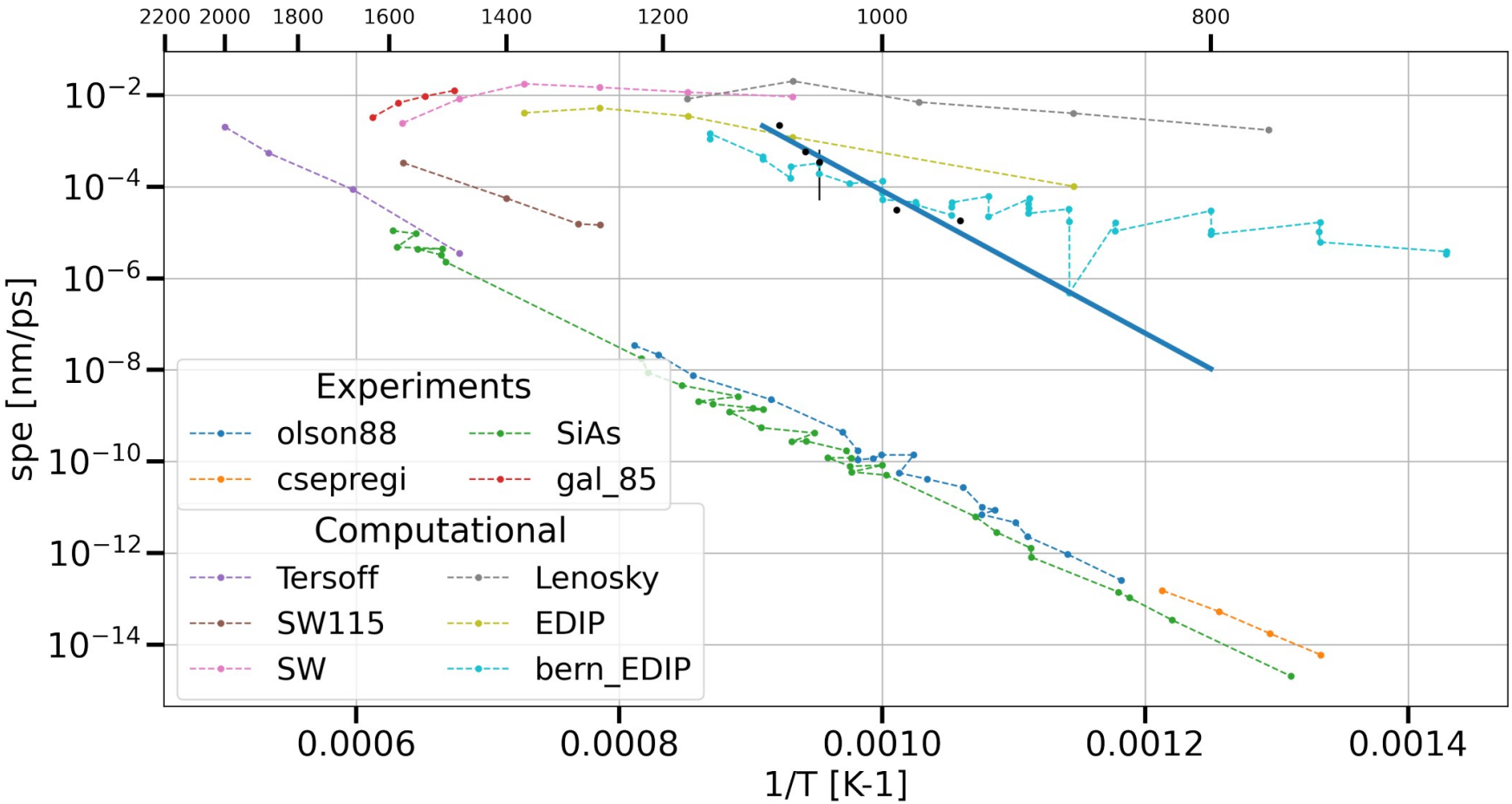

panna: 3.15 eV, experiments[1]: 2.73 eV

[1] Olson and Roth 1988.

Conclusion and outlook

- NN potentials are a valid way to model physical phenomena at the atomistic level
- As a byproduct, PBE-sol xc-functional is not suitable to study thermal related phenomena in silicon
- We are obtaining a correct energy barrier for SPE with pure ab-initio data.

- Improve the amorphous quality
- Isolate the main events for SPE
- Develop a better KMC model.

Emine Kucukbenli

Ruggero Lot

Yusuf Shaidu

Franco Pellegrini

Stefano de Gironcoli